2007 78

THE UNIVERSITY OF NEW SOUTH WALES SCHOOL OF SAFETY SCIENCE

ELECTROSTATIC ENHANCEMENT OF WATER SPRAYS FOR COAL DUST SUPPRESSION

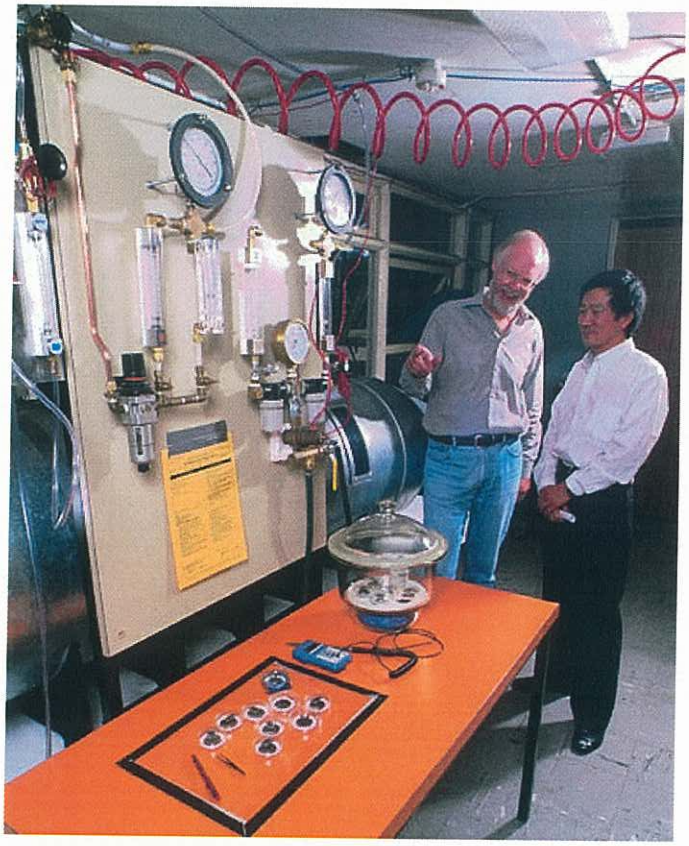

Final Project Report

by

JA Cross, JCW Fowler & Gui Fu

Issued: August 2003

ISBN 0 7334 2058 3

The Health and Safety Trust Research Report

This page intentionally blank

Final report to	:	The Health and Safety Trust
End of grant report	:	The electrostatic enhancement of water sprays for coal dust suppression
Total expended on project	:	$97,300
Project leader	:	JA Cross Professor of Safety Science School of Safety Science The University of New South Wales Sydney NSW 2052
Report prepared by	:	JA Cross JCW Fowler Gui Fu School of Safety Science The University of New South Wales Sydney NSW 2052
Date of issue	:	31 August 2003

This page intentionally blank

ABSTRACT

The overall aim of the Dust Suppression Project is to develop a system to improve airborne dust control based upon electrostatically charged water sprays. The benefits of reduced airborne dust levels will be a lesser risk of occupational lung disease, improved working conditions and, in the case of coal and other potentially explosive dusts, a reduced explosion risk.

Design constraints for a practical and safe electrostatically charged water spraying system, suitable for industrial applications such as mounting on a longwall shearer in an underground coal mine, were identified and design criteria for efficient dust suppression defined. Induction charging was identified as the preferred method of charging and air atomisation as the preferred atomisation technique.

Two items of laboratory testing equipment were developed: the Electrostatically Charged Water Spray Collection (ECWSC) Rig, an apparatus to investigate the properties of electrostatically charged water sprays, and the Electrostatically Charged Water Spray Dust Suppression (ECWSDS) Rig, an apparatus to investigate the ability of electrostatically charged water droplets to capture airborne dust.

An extensive programme of experiments employing an induction-charged air-atomising nozzle was undertaken. The results were used to validate a new theory that had been developed to predict the behaviour of such nozzles. It was also demonstrated that the induction-charged air-atomising nozzle is able to impart a significant electrostatic charge onto water droplets and that unsuppressed coal dust, both inspirable and respirable, can be almost halved by the addition of electrostatic charge to water sprays. Furthermore, it was shown that an electrostatically charged water spraying system can be operated safely in an environment of wet coal dust.

The tasks and objectives of the project were achieved. Further work is to be undertaken to investigate the effectiveness of electrostatically charged water spray in capturing dusts other than coal. In addition, a prototype electrostatically charged water spray system is to be designed, built and demonstrated in field trials, preferably on a longwall shearer in an underground coal mine.

This page intentionally blank

CONTENTS

FIGURES

TABLES

1 SUMMARY

1.1 INTRODUCTION

Dust disease amongst workers employed in the Australian extractive industries has been of concern for very many years.

While the incidence of both silicosis and pneumoconiosis in the extractive industries appears to be declining, presumably due to the enforcement of exposure controls, it is of concern that the application of ever more productive machines to the winning, transportation and comminution of coal and rock is resulting in the generation of greater dust concentrations. Unless innovative methods of dust control are introduced, it may well be that the recent improvements in the incidence of silicosis and pneumoconiosis will not be sustained and may even be reversed.

In New South Wales underground coal mines, for example, dust control on longwall faces improved markedly during the 1980s as evidenced by the improved compliance with statutory exposure limits for airborne respirable dust. Since the early 1990s, however, the incidence of non-compliance on longwall faces has increased. It is more than three times that of other underground coal mining operations and, consequently, the potential exposure of longwall personnel to airborne respirable dust is a cause for concern.

The main reason for this situation is the increasing productivity of the principal item of coal cutting equipment, the longwall shearer. More coal is being won per unit time and, consequently, more dust is being created and is becoming airborne. A second factor that influences levels of airborne dust is the tendency towards greater mining heights. Ventilation air flow often cannot be increased in proportion to the increase in extraction height and, consequently, the degree of dilution of airborne dust is reduced. A third factor may be a higher prevalence of bi-directional shearing and the attendant difficulty, when this technique is employed, of positioning members of the longwall crew clear of the dust stream.

Traditional technologies for suppressing airborne dust have probably reached the limits of their development and new, innovative methods of control are required. An example of such a technology is the electrostatically charged water spraying device for capturing airborne dust currently under development by The University of New South Wales School of Safety Science.

1.2 PROJECT OBJECTIVES AND OUTLINE

The aim of the Dust Suppression Project is to develop a system to improve airborne dust control based upon electrostatically charged water sprays. The benefits of reduced airborne dust levels will be a lesser risk of occupational lung disease, improved working conditions and, in the case of coal and other potentially explosive dusts, a reduced explosion risk.

The project has been divided into three main stages. Stage 1, a feasibility study into the application and potential for electrostatically charged water sprays at the coal face in underground mines, was funded by a grant under the National Energy Research, Development and Demonstration (NERD&D) Programme. Work commenced in 1992 and was completed early in 1994. It is described in detail in the first interim report[1], issued in April 1994.

Stage 2 is described in this report. It was funded by Australian Coal Research Limited, under the Australian Coal Association Research Program, and by The Health and Safety Trust (the former Joint Coal Board Health and Safety Trust). In addition, a grant to partially defray the cost of the basic research element of the project was awarded to the School of Safety Science by The University of New South Wales on behalf of the Australian Research Council.

The overall objective of Stage 2 of the Dust Suppression Project was to develop and employ a laboratory facility to investigate the effects of the principal design and operational variables of an electrostatically charged water spraying system on dust suppression efficiency. Specific tasks undertaken as part of the work described in this report included the following.

- Evaluating the feasibility of electrostatic dust suppression by assessing likely acceptance by industry, equipment manufacturers and regulatory authorities.
- Identifying the safety issues which are particular to electrostatic dust suppression.
- Defining the optimum design features for a charged water sprayer.
- Building a laboratory test facility to verify the design parameters.
- Constructing an electrostatically charged water spraying device.
- Testing the effects of the design parameters on the charging of water sprays.
- Testing the effects of the design parameters on coal dust capture.
- Assessing the effectiveness in capturing coal dust of a charged spray of optimum design against an uncharged spray.

The aim of Stage 3 of the Dust Suppression Project will be to determine whether the concept of dust capture by electrostatically charged water sprays can be applied to dusts other than

[1] Cross, JA & Smith, P 1994, Electrostatic enhancement of water sprays for coal dust suppression (Interim Project Report, The University of New South Wales Department of Safety Science), Australian Coal Association Research Program Final Report, Project No. C1621, available Brisbane: Australian Research Administration Pty Ltd

coal and to demonstrate the technology in field trials. Specific tasks to be undertaken include the following.

- Testing the effectiveness of electrostatically charged water spray in capturing dusts other than coal.
- Designing and constructing an electrostatically charged water spraying system that is suitable and safe for industrial use, particularly at the coal face in underground mines.
- Undertaking a feasibility study and risk assessment into the application of such a system at the coal face.
- Demonstrating the prototype system in field trials, preferably on a longwall shearer in an underground coal mine.

1.3 MAIN FINDINGS AND CONCLUSIONS

The objectives of Stage 2 of the Dust Suppression Project, described in this report, have been achieved. The principal findings are outlined below.

1.3.1 Design constraints and criteria

As the result of an extensive programme of consultation with industry, equipment manufacturers and regulatory authorities, design issues and constraints were identified for a practical and safe electrostatically charged water spraying system, suitable for industrial applications such as mounting on a longwall shearer in an underground coal mine. A set of design criteria for efficient dust suppression was drawn up and a safety assessment undertaken. Induction charging was identified as the preferred charging technique and air atomisation as the preferred atomisation technique.

1.3.2 Spraying systems

Sources of electrostatically charged spraying systems that had been developed for electrostatic operation were identified and a list of commercially available equipment was drawn up. It was considered, however, that none of these adequately fulfilled the design constraints and criteria. Consequently, it was decided that electrostatic charging functionality would be added to a commercial, non-electrostatic spraying system. A list of sources of non-electrostatic systems that had the potential to be adapted was compiled, the devices assessed and a preferred device selected.

1.3.3 Development of induction charging and atomisation theories

Because of the complexity of the induction charging / air atomisation process and the large number of parameters which could potentially effect its efficiency, a rigorous theory with

which to guide the laboratory investigations and design process was essential. However, following an extensive review of the literature, existing theories for the induction charging and air atomisation of a liquid jet were found to be inadequate. Consequently, new theories were developed which describe the charging of a liquid jet by induction and the hydrodynamics of liquid jet disintegration under the influence of atomising air.

This task was additional to the original scope of Stage 2 of the Dust Suppression Project.

1.3.4 Laboratory testing

An item of laboratory test equipment, the Electrostatically Charged Water Spray Collection (ECWSC) Rig was designed and constructed in order to facilitate the testing of electrostatically charged water spraying devices and the measurement of spray current and spray cloud parameters. In addition, a second major item of laboratory equipment, the Electrostatically Charged Water Spray Dust Suppression (ECWSDS) Rig, was developed for the purpose of investigating the ability of electrostatically charged water droplets to capture airborne coal dust.

The induction-charged air-atomising nozzle that had been selected as the preferred device was employed in a preliminary series of experiments which was undertaken using the ECWSC Rig. The primary objective, the validation of the newly developed theory, was achieved. It was also demonstrated that the induction-charged air-atomising nozzle is able to impart a significant electrostatic charge onto water droplets.

The ECWSDS Rig was employed in an extensive series of experiments that investigated the effects of the principal design and operational variables on dust suppression efficiency. It was demonstrated that unsuppressed coal dust, both inspirable and respirable, can be almost halved by the addition of electrostatic charge to the water spray. Furthermore, it was shown that an electrostatically charged water spray dust suppression system can be operated safely in an environment of wet coal dust.

2 INTRODUCTION

2.1 BACKGROUND

Dust disease amongst workers employed in the Australian extractive industries has been of concern for very many years.

While the incidence of both silicosis and pneumoconiosis in the extractive industries appears to be declining, presumably due to the enforcement of exposure controls, it is of concern that the application of ever more productive machines to the winning, transportation and comminution of coal and rock is resulting in the generation of greater dust concentrations. Unless innovative methods of dust control are introduced, it may well be that the recent improvements in the incidence of silicosis and pneumoconiosis will not be sustained and may even be reversed.

Dust control is a significant issue in underground coal mining. In New South Wales underground coal mines, for example, dust control on longwall faces improved markedly during the 1980s as evidenced by the improved compliance with statutory exposure limits for airborne respirable dust. Since the early 1990s, however, the incidence of non-compliance on longwall faces has increased. It is more than three times that of other underground coal mining operations and, consequently, the potential exposure of longwall personnel to airborne respirable dust is a cause for concern.

The main reason for this situation is the increasing productivity of the principal item of coal cutting equipment, the longwall shearer. More coal is being won per unit time and, consequently, more dust is being created and is becoming airborne. A second factor that influences levels of airborne dust is the tendency towards greater mining heights. Ventilation air flow often cannot be increased in proportion to the increase in extraction height and, consequently, the degree of dilution of airborne dust is reduced. A third factor may be a higher prevalence of bi-directional shearing and the attendant difficulty, when this technique is employed, of positioning members of the longwall crew clear of the dust stream.

The primary benefit of dust suppression in underground coal mines is one of occupational health: reducing the exposure of miners to the respirable fraction of coal dust which may lead to lung disease. Secondary benefits are ones of safety: reducing the risk of explosion and improving working conditions by reducing the total amount of airborne coal dust.

Traditional technologies for suppressing airborne dust have probably reached the limits of their development and new, innovative methods of control are required. An example of such a technology is the electrostatically charged water spraying device for capturing airborne dust currently under development by The University of New South Wales School of Safety Science.

2.2 OBJECTIVES

The aim of the Dust Suppression Project is to develop a system to improve airborne dust control based upon electrostatically charged water sprays. The benefits of reduced airborne dust levels will be a lesser risk of occupational lung disease, improved working conditions and, in the case of coal and other potentially explosive dusts, a reduced explosion risk.

The project has been divided into three main stages. Stage 1, a feasibility study into the application and potential for electrostatically charged water sprays at the coal face in underground mines, was funded by a grant under the National Energy Research, Development and Demonstration (NERD&D) Programme. Work commenced in 1992 and was completed early in 1994.

Stage 2, described in this report, has been funded by Australian Coal Research Limited, under the Australian Coal Association Research Program, and by The Health and Safety Trust (the former Joint Coal Board Health and Safety Trust). In addition, a grant to partially defray the cost of the basic research element of the project was awarded to the School of Safety Science by The University of New South Wales on behalf of the Australian Research Council.

The overall objective of Stage 2 of the Dust Suppression Project was to develop and employ a laboratory facility to investigate the effects of the principal design and operational variables of an electrostatically charged water spraying system on dust suppression efficiency. Specific tasks undertaken as part of the work described in this report included the following.

- Evaluating the feasibility of electrostatic dust suppression by assessing likely acceptance by industry, equipment manufacturers and regulatory authorities.
- Identifying the safety issues which are particular to electrostatic dust suppression.
- Defining the optimum design features for a charged water sprayer.
- Building a laboratory test facility to verify the design parameters.
- Constructing an electrostatically charged water spraying device.
- Testing the effects of the design parameters on the charging of water sprays.
- Testing the effects of the design parameters on coal dust capture.
- Assessing the effectiveness in capturing coal dust of a charged spray of optimum design against an uncharged spray.

The aim of Stage 3 of the Dust Suppression Project will be to determine whether the concept of dust capture by electrostatically charged water sprays can be applied to dusts other than coal and to demonstrate the technology in field trials.

2.3 PROJECT REPORTS

The first interim report (Cross & Smith 1994) described the first stage of the Dust Suppression Project. The second interim report (Cross, Fowler & Xiao 1998) described the work undertaken in the period between July 1994 and June 1997 as part of Stage 2 of the Dust Suppression Project and funded by Australian Coal Research Limited, under the Australian Coal Association Research Program.

This third interim report describes the whole of the Stage 2 work and largely supersedes Cross, Fowler and Xiao (1998).

2.4 CONSULTATION WITH INDUSTRY

One of the first tasks of Stage 2 was the identification of design issues and constraints for a practical and safe electrostatically charged water spraying (ECWS) system suitable for use in the extractive industries. A longwall shearer, the principal item of coal cutting equipment employed in underground coal mines, was selected as the initial application as it was anticipated that, although the operating environment was onerous, the potential benefits of improved dust suppression were substantial.

In order to define the constraints imposed by the industrial environment, discussions took place with appropriate personnel. These included representatives of mining and quarrying companies, equipment manufacturers and regulatory authorities. During the discussions, the existing spray arrangements for dust suppression were considered in detail.

Based upon the advice received, it was concluded that the following design issues and constraints would have to be addressed if electrostatically charged water spraying for dust suppression was to gain acceptance.

a. An ECWS system should not employ 'excessively high' voltages.
b. The system must 'fail safe'.
c. Electrostatic charge must not accumulate upon the equipment, upon personnel or upon the surroundings.
d. An ECWS system should be at least as robust and durable as conventional water spray systems.
e. The system should not require more maintenance than conventional water spray systems.
f. The system should be capable of being retrofitted to existing equipment.
g. An ECWS system must be capable of utilising 'grey' water.
h. The system should operate at or below the water pressure supplied to conventional water spray systems.
i. An ECWS system must meet regulatory requirements regarding explosion protection when employed in potentially explosive gas atmospheres.

In the particular case of coal mining, additional issues were identified.

a. Where a 'shearer clearer', a device to confine dust to the coal face side of the longwall shearer, is fitted, an ECWS system should not detract from its efficacy.

b. In areas of mines having soft floor, it is desirable that an ECWS system employ less water than conventional water spray systems.

2.5 DESIGN CRITERIA

Insight into the design criteria for efficient dust suppression has been provided by the numerical modelling of the process of dust capture by electrostatically charged water droplets carried out as Stage 1 of the Dust Suppression Project (Cross & Smith 1994).

2.5.1 Droplet size

Droplet diameters in the range 10 to 320 μm were simulated during the numerical modelling and it was demonstrated that the effectiveness of dust particle capture by charged water droplets increases markedly with decreasing droplet size. Consequently, a goal of the spray-charger development was identified to be the ability to generate charged water droplets of a diameter that is at the lower end of this range.

For purposes of comparison, ranges of water spray droplet sizes generated by commercially available spraying devices are given in table 2.1.

Table 2.1 Water spray droplet sizes generated by commercially available devices

Atomisation process	*Spray pattern*	*Range of water spray droplet sizes (volume median diameter)*
		μm
Hydrostatic	Full cone	50 - 2000
	Flat fan	20 - 1500
	Hollow cone	1 - 1000
Pneumatic	Full cone	0.1 - 500
Centrifugal	Flat disk	50 - 200
	Hollow cone	

Because of the plethora of available spraying devices, the values in the table must be viewed as merely indicative. They serve, however, to illustrate the general tendency for pneumatic devices to generate finer droplet sizes than purely hydrostatic ones.

2.5.2 Droplet charge

When a liquid droplet is charged, the charge resides on the surface and exerts an outward force that tends to counteract the surface tension. A sufficiently high charge would result in the electrostatic force exceeding the surface tension and, as a consequence, the droplet would explode. The point at which the electrostatic and surface tension forces just balance is known as the Rayleigh charge limit.

Levels of electrostatic charge in the range 1 to 32 percent of the Rayleigh charge limit were simulated during the numerical modelling and it was demonstrated that the effectiveness of dust particle capture by charged water droplets increased with increasing droplet charge. Consequently, a spraying device that will generate a high droplet charge was identified as a goal of spray-charger development.

2.5.3 Water flowrate

Water flowrates in the range 10 to 320 L/min (167 to 5330 mL/s) were simulated during the numerical modelling and it was demonstrated that the effectiveness of dust particle capture by charged water droplets increased markedly with increasing flowrate. A spraying device with a throughput of this order was identified as one of the aims of spray-charger development, provided that this did not result in a low droplet charge.

2.5.4 Interaction time between dust particles and water droplets

Interaction times between dust particles and water droplets in the range 0.5 to 4.0 seconds were simulated during the numerical modelling and it was demonstrated that the effectiveness of dust particle capture by charged water droplets increased markedly with increasing interaction time. It may well be that interaction time can be maximised by directing the spray parallel with, rather than perpendicular to, the flow of dusty air.

2.5.5 Spray velocity and geometry

In the case of uncharged droplets, the numerical modelling demonstrated that initial spray velocity was a significant factor in the effectiveness of dust particle capture. In the case of uncharged droplets, however, initial spray velocity was believed not to be of significance in dust particle capture. It is, of course, important to ensure that charged droplets leaving the electrostatically charged water spraying device do so with sufficient forward momentum to overcome the charged droplet field and reach the air cleaning zone. Consideration may have to be given to providing 'air assistance' to the charged droplets in order to accelerate them after they leave the spraying device.

2.6 POTENTIAL SPRAYING DEVICES

In discussions with representatives of manufacturers and research establishments, both in Australia and in the United Kingdom, several commercially available electrostatically charged liquid spraying devices were identified together with those non electrostatic devices which it was anticipated would offer the possibility of being adapted for electrostatic charging.

2.6.1 Physical processes

The various physical processes embodied in the devices are explained below.

2.6.1.1 The atomisation process

Relevant practicable means of atomising a liquid to form a spray were all identified as falling into one of four categories.

a. High speed rotary atomisers of the type used in automated paint spraying booths in factories. In this category of device, atomisation is created by a combination of mechanical and electrostatic forces. The most recent developments of these devices are designed for water-based paints and may, at least in theory, atomise pure water.

b. Hydrostatic atomising spray nozzles in which high pressure (of the same order as that utilised in industrial hydraulic circuits) is employed to atomise a liquid through a very small orifice.

c. Pneumatic atomising spray nozzles in which liquid exiting from the tip of a nozzle at relatively low pressure as a continuous stream is atomised by a coaxial air jet impinging on it.

d. Hybrid devices employing both hydrostatic and pneumatic atomisation.

Each of these methods of atomisation has found application in commercial electrostatically charged liquid spraying systems.

2.6.1.2 The charging process

Relevant practicable means of applying electrostatic charge to the liquid spray were all based upon one of three physical principles.

a. Contact charging, where the atomising device is itself raised to a sufficiently high direct current electrical potential for charge transfer by conduction to a liquid to occur.

b. Corona charging. A sufficiently high electrical potential is applied to a needle located in the zone of atomisation for dielectric breakdown of the air immediately surrounding the needle point to result. Droplets travelling through this ionised-field region become charged by ion attachment.

c. Electrostatic induction charging. An electrical potential is applied to an electrode immediately adjacent to the zone of atomisation. Provided that the liquid has some conductivity, however small, an excess charge of opposite polarity will accumulate on the surface of the liquid and individual droplets formed at this surface will themselves carry a net charge.

Each of these three methods of charging has found application in commercial electrostatically charged liquid spraying systems.

Figure 2.1 presents a generalised geometry with which to illustrate the various methods of electrostatic charging. Although a hydrostatic atomising spray nozzle is employed for the purposes of illustration, it must be understood that the methods of charging may be used in association with other atomisation techniques.

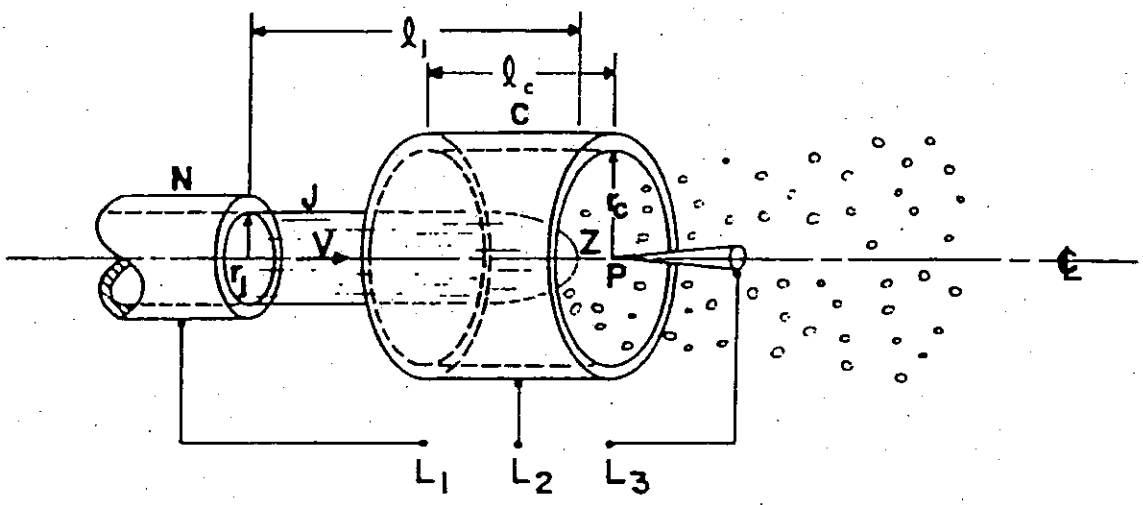

Fig. 2.1 Generalised geometry for electrostatic spray charging (after Law 1978)

Contact charging. Charge transfer by conduction to the liquid jet (and hence to the spray droplets as they form) can be effected by connecting conductor L_1 to a voltage source in order to provide an excess supply of free charge. However, for conductive liquids, maintenance of the conductor L_1 at an elevated voltage requires electrical isolation of the liquid by means of a 'voltage breaking' device (sec. 2.6.1.3).

Corona or ionised-field charging. If conductors L_1 and L_2 are connected to earth and a sufficiently high electrical potential applied to conductor L_3, dielectric breakdown of the air immediately surrounding the needle point P will result. Consequently, a self-sustaining gaseous discharge current will flow between P and the electrode C and spray droplets travelling through this zone will become charged by ion attachment.

Electrostatic induction charging. If a potential is applied to the cylindrical electrode C by connection of a voltage source between conductors L_1 and L_2, an excess charge of opposite polarity to that of L_2 will accumulate on the earthed jet J owing to the electrostatic induction of electrons onto or away from the surface of the jet in order to maintain it at earth potential in the presence of the nearby charged electrode. Spray droplets formed from the charged jet will themselves carry a charge of the same polarity as the jet.

Two factors of potential practical significance follow from the above.

a. In the case of both contact and induction charging, electrostatic charge is applied to the liquid and then transferred to the spray droplets as then are formed. Conversely, in the case of corona charging, the charge is applied to the droplets themselves.

b. Contact and corona charging result in a spray charge of the same polarity as the charging electrode whereas induction charging leads to a spray charge of the opposite polarity.

2.6.1.3 'Voltage breaking'

Clearly, any spray charging system will cease to function if the voltage source is directly connected to earth and where the liquid to be sprayed is water, a conducting liquid, a potential pathway exists from the charged electrode to earth via the water supply.

In the case of contact charging, where the electrode is in direct contact with the liquid supply, a 'voltage breaking' device is necessary in order to isolate the liquid circuit in the vicinity of the charging device from earth.

Devices that have been adopted or postulated in order to isolate the supply of a conducting liquid from earth but still permit continuous charging/spraying include the following.

a. A switched liquid supply employing two or more tanks which are themselves isolated from earth and refilled via an isolation valve arrangement.

b. An arrangement whereby the conducting liquid flows through a sufficiently long length of insulated small bore tubing to raise the electrical resistance of the liquid supply to a sufficiently high value for compatibility with the voltage source.

c. The introduction of air bubbles or 'slugs' of insulating fluid into the supply line in order to interrupt the conductivity of the liquid column (Cross & Smith 1994).

d. The incorporation of a 'peristaltic' device into the supply line in order to render the liquid column discontinuous.

In the case of corona charging, where the electrode is not in direct contact with the liquid supply, the incorporation of a 'voltage breaking' device is unnecessary. For induction charging, however, the clearance between electrode and liquid is, of necessity, very small and 'voltage breaking' may be necessary in order accommodate intermittent contact.

2.6.2 Electrostatically charged liquid spraying devices

Manufacturers of electrostatically charged liquid spraying devices were identified. They are listed in table 2.2 together with the characteristics of the devices that they offer.

Table 2.2 Commercially available electrostatically charged liquid spraying devices

Manufacturer	*Australian importer/ distributor/ supplier*	*Industry sector*	*Atomisation process*	*Charging process*	*'Voltage breaking'*
Behr Industrie-anlagen	–	Paint spraying	Centrifugal Centrifugal	Contact Ionisation	Yes N/A
Binks-Bullows Limited/ Sames SA	Binks-Bullows (Aust) Pty Limited	Paint spraying	Pneumatic Hydrostatic Centrifugal Centrifugal	Ionisation Ionisation Contact Ionisation	N/A N/A Yes N/A
Dete Sprintz- und Lackier-systeme GmbH	Dete (Aust.) Pty Ltd Gyozo Pty Ltd	Paint spraying	Hydrostatic?	Ionisation	N/A
Eltex-Elektrostatik-Gesellschaft mbH	B.K. Sales Pty Ltd	Printing	Hydrostatic Electrostatic	Ionisation	N/A
Graco Inc.	Graco Inc.	Paint spraying	Hydrostatic	Ionisation	N/A
ITW Finishing Systems & Products Group (DeVilbiss Ransberg Gema Volstatic)	ITW Finishing Systems & Products Pty Ltd	Paint spraying	Pneumatic Hydrostatic Centrifugal Centrifugal	Ionisation Ionisation Contact Ionisation	N/A N/A Yes N/A
Kremlin SA (Exel Group)	Epac Productions	Paint spraying	Pneumatic Hydrostatic Centrifugal	Ionisation Ionisation –	N/A N/A –
Nordson Corporation	Nordson Australia Pty Ltd	Paint spraying	Pneumatic Hydrostatic Centrifugal Centrifugal	Ionisation Ionisation Contact Ionisation	N/A N/A Yes N/A
Wagner GmbH?	Wagner Spray-tech Australia Pty Ltd	Paint spraying	Hydrostatic	Ionisation	N/A

2.6.3 Non electrostatic liquid spraying devices

Manufacturers of non electrostatic liquid spraying devices which have the potential to be adapted were identified. They are listed in table 2.3 together with the characteristics of the devices that they offer.

Table 2.3 Commercially available non-electrostatic liquid spraying devices

Manufacturer	*Australian importer/ distributor/ supplier*	*Industry sector*	*Atomisation process*	*Comments*
Anest Iwata Corporation	Cormack Anest Iwata Pty Ltd	Paint spraying	Pneumatic Hydrostatic	–
Arag s.r.l.	–	Agriculture	Hydrostatic	–
Bete Fog Nozzle Inc.	Sprayflo Pty Ltd	General	Pneumatic Hydrostatic	
Bex s.a.	Sprayflo Pty Ltd	–	–	–
Conflow Limited	Senior Australia Limited	Coal mining	Hydrostatic	–
Delavan-Delta Inc.	Spray Nozzle Engineering Pty Ltd	General	Pneumatic Hydrostatic	–
Dust Suppression Australasia Pty Ltd	–	Minerals	Hydrostatic	Dust suppression systems
Ecco Finishing AB	None	Paint spraying	Pneumatic Hydrostatic	–
ITW Vortec (ITW Finishing Systems & Products Group)	ITW Finishing Systems & Products Pty Ltd	–	Pneumatic	–
Lechler GmbH + Co KG	Strauff Corporation Pty Ltd	General	Pneumatic Hydrostatic	–
Spraying Systems Co.	Spraying Systems Australia Pty Ltd	General	Pneumatic Hydrostatic	Have been adapted for electrostatic crop spraying
Uni-Spray Nozzles Inc.	–	–	–	–

2.6.4 Device selection

2.6.4.1 Electrostatic devices

The commercially available electrostatically charged liquid spraying devices outlined in table 2.2 were examined against the design issues and constraints set out in section 2.4 and the design criteria set out in section 2.5. Unfortunately, however, none of the devices satisfied all of the design issues and met all of the constraints, nor were they capable of being appropriately adapted.

Firstly, the methods of charging presented potential problems. Most of the devices employed ionisation (corona) charging at an electrical potential of the order of 100,000 volts. This was considered to be at variance with industry's perceived requirement that the system not employ 'excessively high' voltages and also gave rise to doubts as the possibility of meeting regulatory requirements with respect to explosion protection in potentially explosive gas atmospheres. In addition, the presence of a charging 'needle' in the spray cloud immediately in front of the atomisation device, an essential feature of corona charging, was considered a potential design problem in terms of the robustness and durability of the device.

While the remaining devices used contact charging, they employed an elevated electrical potential of the same order as that used for ionisation charging. However, the whole device was, of necessity, raised to this potential and it was considered probable that the inevitable high capacitance would preclude its meeting explosion protection requirements. Although the absence of the vulnerable charging 'needle' was an advantage of such devices, they would definitely require 'voltage breaking' (sec. 2.6.1.3).

Unfortunately, none of the devices employed induction charging which appeared to be the process most likely to comply with the design constraints (sec. 2.4).

Secondly, the atomisation process employed in some of the devices presented potential design problems. Several employed centrifugal atomisers operating at speeds of the order of 50,000 rpm and were sensitive to shock & vibration raising issues of robustness and durability. Others employed hydrostatic atomisation at pressures similar to those in industrial hydraulic circuits. These failed to meet the pressure design constraint (sec. 2.4) in that they required pressure intensification compared with that supplied to conventional water spray systems employed for dust suppression. In addition, the combination of high water pressures, small orifices and 'grey' water raised potential design issues such as excessive nozzle wear and blocked nozzles.

The pneumatic atomisation process utilised in a few of the devices was considered to offer several potential advantages in that it employed much lower water pressures and larger orifice

sizes that the equivalent hydrostatic process. In addition, the required pressure range for the supply of atomising air was well within that of reticulated industrial compressed air supplies. It was also considered that the comparatively larger orifice sizes and lower liquid nozzle velocities might well reduce, but by no means obviate, problems of nozzle wear and blockage. Unfortunately, however, none of the devices used pneumatic atomisation and induction charging in combination.

In summary, it was considered that none of the electrostatically charged liquid spraying devices outlined in table 2.2 was appropriate, in its original form, for use in dust suppression in industrial applications such as underground coal mines and, furthermore, than none was suitable for such adaptation.

2.6.4.2 Non electrostatic devices

A range of non electrostatic liquid spraying devices as outlined in table 2.3 was examined from the point of view of their potential to be so adapted, together with their potential compliance with the design issues and constraints set out in section 2.4. Devices that employed hydrostatic atomisation utilised pressures similar to those in industrial hydraulic circuits and were rejected for the reasons outlined above. Devices which employed the pneumatic atomisation process but had been specifically designed for the purpose of paint spraying were not considered further as they had been optimised for that purpose and appeared to offered little potential for adaptation.

It was considered that 'general purpose' air-atomising nozzles, which could be adapted for induction charging, offered the most potential. These were readily available in a wide range of materials and of orifice shapes & sizes. A characteristic of such nozzles, of particularly value during the laboratory optimisation phase of the research, was that spray droplet size can be adjusted by varying the atomising air pressure.

2.6.4.3 The preferred device

The induction-charged air-atomising nozzle was the preferred device. The reasons for its selection are summarised as follows.

a. It operates at a relatively low voltage (of the order of 1000 volts) which makes its acceptance by industry and its introduction into hazardous areas such as a coal face less problematical.

b. The relatively low power supply drain current and voltage increase the probability of the system being able to satisfy explosion protection requirements.

c. The relatively low voltage requires only a simple power supply.

d. The 'non-contact' nature of the device and its relatively low voltage increase the probability of its being able to be operated either without 'voltage breaking' or with a simple 'voltage breaking' device.

e. It employs water and air at 'normal industrial pressures'.

f. The process of air atomisation produces the small spray droplet sizes which numerical modelling had indicated to be the most effective in dust capture (Cross & Smith 1994). In addition, droplet size can be adjusted by varying the atomising air pressure.

g. The device is more robust than many of the alternatives.

h. The comparatively larger orifice sizes and lower liquid nozzle velocities compared with the hydrostatic nozzles employed in conventional industrial water spraying devices might well reduce maintenance requirements.

i. It was envisaged that the task of retrofitting such a device to existing equipment would be no more difficult than for many of the alternative devices.

2.7 SAFETY ISSUES PARTICULAR TO ELECTROSTATIC DUST SUPPRESSION

A detailed investigation into the risks of electrostatic dust suppression in potentially hazardous areas in underground coal mines will be undertaken during Stage 3 of the Dust Suppression Project. In the analysis, the potential risks of electrostatic operation, if any, will be assessed against the reduction of risk of occupational lung disease and explosion as a result of a reduced dust level.

Because of the possible presence of methane in potential coal mining applications and, consequently, of an explosive gas atmosphere, an important requirement is that no electrical spark be generated that could constitute an ignition source. In order to ignite a stochastic mixture of methane in air, the generally accepted minimum energy is 0.28 mJ (Cross 1987). Consequently, it is essential either that no electrical spark occur or that the energy of any spark not exceed this figure.

There are a number of potential sources of sparks that must be considered. These include the following.

- The elevated voltage spray charging electrode and cables
- The elevated voltage power supply
- Lightning type discharges
- Electrical coronas
- Charge accumulation upon isolated objects

2.7.1 Elevated voltage electrode and cables

An elevated voltage electrode is required to charge the spray. It may be postulated that a short circuit will occur at some point in time and, consequently, it is essential that the ensuing spark be of insufficient energy to ignite a mixture of methane in air. It is probable that this requirement will be most appropriately satisfied by ensuring that the elevated voltage electrode and cables comply with Australian/New Zealand Standard AS/NZS 60079.11:2000 *Electrical apparatus for explosive gas atmospheres–Part 11: Intrinsic safety 'i'*.

2.7.2 Power supply

An important requirement is that the power supply be explosion protected. It is probable that this requirement will be most appropriately satisfied by enclosing the power supply in a flameproof enclosure in accordance with Australian/New Zealand Standard AS/NZS 60079.1:2002 *Electrical apparatus for explosive gas atmospheres–Part1: Flameproof enclosure 'd'*.

2.7.3 Lightning type discharges

It can be postulated that a charged cloud of droplets could theoretically discharge together and ignite a mixture of methane in air, the mechanism being similar to a flash of lightning from a charged thunder cloud. However, for this to occur the following requirements would need to be met.

a. The total stored energy present in the cloud of droplets in a spray would need to exceed 0.28 mJ.

b. The electric field would need to be sufficient to cause the air to breakdown and allow the charge on the droplets to dissipate in a single spark.

The possibility of lightning type discharges occurring on a small scale was studied extensively in the early 1970s during investigations into the causes of supertanker explosions during washing out operations. The results of this theoretical research indicated that such discharges do not occur, even on the scale of a tank in a supertanker. There is no suggestion that such sparks might ever have occurred in practice (Cross 1987).

2.7.4 Electrical coronas

The electric field will intensify around metal objects especially if they are of low radius of curvature. However localised strong electric fields, if they exceed 3 million volts/metre and hence cause air breakdown, are more likely to result in electrical coronas than in lightning discharges.

Electrical coronas are localised electrical breakdowns of air that may occur when an earthed object is subjected to an electric field. They form a source of ions (molecules with an additional electron or one electron short) that then travel away from the source. Electrical coronas generate far less energy than sparks but they do generate some heat, both in the air and at the metal. Corona discharges are generally considered to be non incendive.

The ions created in an electrical corona would tend to discharge the charged droplets and, consequently, an objective of the spray system design is to avoid any situation that might create them. The issue of corona discharge is considered in detail in sections 3.2.3, 4.8 and 5.2.1.2.

2.7.5 Isolated charged objects

If a charge builds up on an isolated object, then, when its isolation is reduced and it approaches an earth, it may discharge suddenly in a spark. Consequently, it is necessary to ensure that insufficient charge builds up on any object to cause a spark of greater energy that the minimum ignition energy of a methane in air mixture.

There are two ways in which charge may build up on an isolated object, namely

- induction and
- deposition of charged spray.

2.7.5.1 Induction charging

The strong electric fields created either by the tip of the charging nozzle or by the cloud of charged droplets may induce charge onto objects in the following way. The electric field will attract charge of opposite polarity into any nearby object that is connected to earth. If that object's link to earth is broken, it will retain that charge and could later generate a spark.

An example of possible induction charging is that of a person wearing insulating footwear walking through the strong electric field region and momentarily touching an earthed metal object, thus drawing charge onto themselves from that object. When the person subsequently left the area they would carry a charge that could later cause a spark. However, this risk could be eliminated by the wearing of conductive footwear that would non-hazardously discharge the person the moment they left the strong field region.

In a mining situation in which wet coal dust is generally abundant, it is very unlikely that there would be unearthed conductors. Consequently, it is expected that induction charging risks could be eliminated.

2.7.5.2 Deposition of charged spray

If a sufficient quantity of charged water spray were to be deposited onto an electrically isolated object, it could charge it to a potentially hazardous level such that if the charge were to be suddenly dissipated by a spark, it would generate more than the minimum ignition energy of a methane in air mixture.

There are two ways in which charged spray may deposit on isolated objects, namely

- objects travelling through the spray and
- spray drifting through the mine.

Objects which could travel through the spray include the following:

- personnel walking through the charged spray cloud;
- large water slugs falling through the charged spray cloud; and
- lumps of coal falling through the charged spray cloud.

Charged droplets could drift through the mine, depositing on electrically isolated objects and charging them to potentially hazardous levels. Possible solutions to this issue are to minimise the escape of charged droplets from the immediate spray region or to alternate the polarity of spray between positive and negative. This would mean that the positive mist that escapes from the spray zone would neutralise the negative mist that escapes and thus minimise or obviate any hazardous charge build-up on isolated objects.

2.7.5.3 Elimination of electrically isolated objects

An object is electrically isolated when it is not electrically connected to earth. Although there is no way to earth a falling lump of coal while it is in the air, objects on the ground are normally electrically connected to earth because current flows through them to the ground. The only cases where this does not happen are when either the ground is highly resistive or the object is highly resistive.

Coal, and in particular wet coal, would have sufficient conductivity to allow charge to dissipate. Plastic materials which are highly resistive could pose a hazard. However the precautions taken in coal mines to prevent build up of static charge generated by friction would also prevent build up due to charged spray.

3 EQUIPMENT DEVELOPMENT AND TESTING METHODOLOGY

3.1 SCOPE OF THE PROGRAMME

The equipment development programme comprised the design, construction and commissioning of an electrostatically charged water spraying device, the induction-charged air-atomising nozzle, and two items of laboratory testing equipment.

a. The Electrostatically Charged Water Spray Collection (ECWSC) Rig, an apparatus to investigate the generation of electrostatically charged water sprays.

b. The Electrostatically Charged Water Spray Dust Suppression (ECWSDS) Rig, an apparatus to investigate the ability of electrostatically charge water droplets to capture airborne coal dust.

3.2 DESCRIPTION OF THE INDUCTION-CHARGED AIR-ATOMISING NOZZLE

3.2.1 Introduction

As the preferred electrostatically charged water spraying device, the induction-charged air-atomising nozzle (sec. 2.6.4.3) was chosen for the programme of laboratory testing undertaken during Stage 2 of the Dust Suppression Project.

3.2.2 The air-atomising nozzle

The air-atomising nozzles utilised for the testing programme were selected from the SU22/42 series manufactured by Spraying Systems Co. of Wheaton, Illinois, USA. They were chosen for the following reasons.

a. They were readily available in a wide range of materials and sizes.

b. They had been employed by several research groups investigating the potential for electrostatically charged crop spraying in agriculture and horticulture.

The air-atomising nozzle is illustrated in figure 3.1 below in longitudinal section.

3.2.2.1 Spray characteristics

The SU22/42 series of air-atomising nozzles are designed to operate at 70 to 400 kPa water pressure and 110 to 700 kPa air pressure (Spraying Systems Co. 1994). They produce a 360 degree round spray pattern with an included spray angle of between 17 and 22 degrees. This spray angle is maintained for a distance from the nozzle orifice of between 0.61 and 1.17 metres beyond which the flow becomes turbulent. The total penetration of the spray varies from 4.9 to 9.1 metres. The larger angles and greater distances are associated with higher air pressures.

The range of water flowrates is from 45 to 4170 mL/min (0.75 to 69.5 mL/s) while the volume median diameter (VMD) spray droplet size ranges from 20 to 400 microns, the larger diameters being associated with higher water flowrates.

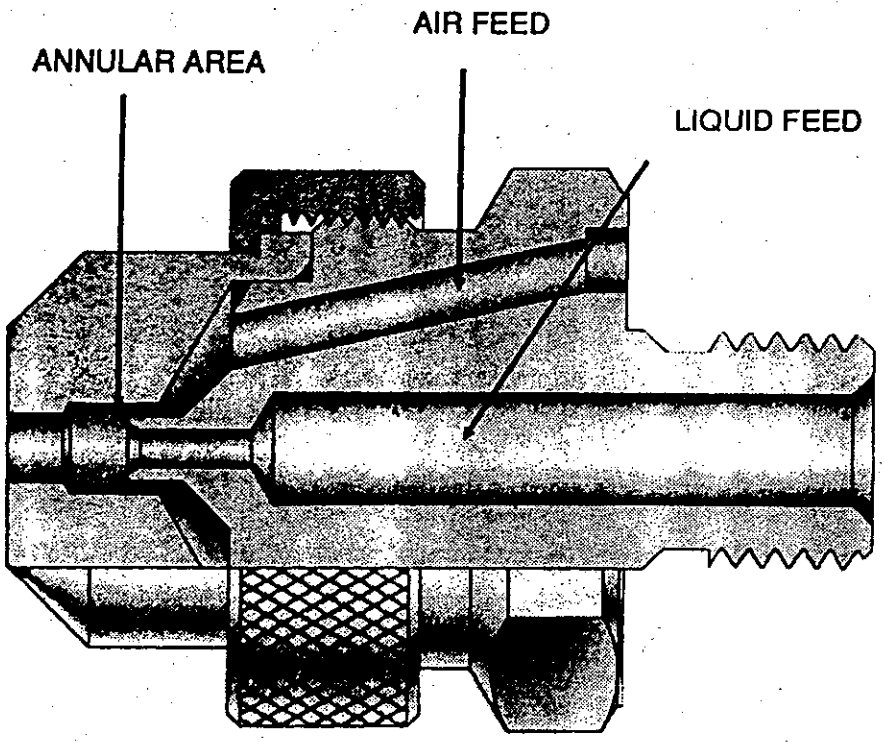

Fig. 3.1 The air-atomising nozzle
(adapted from Spraying Systems Co. 1994)

3.2.3 The induction charging electrode

The concept of the induction-charged air-atomising nozzle is illustrated in figure 3.2 below. The design was based upon that first employed by Law (1978) and subsequently used by several investigators.

The operation of the device is as follows. A continuous water jet emanates from the centrally located nozzle orifice that is at earth potential. A coaxial electrode at elevated potential creates an intense electric field between its surface and that of the nozzle. This electric field polarises the water jet by attracting charge of the opposite polarity to that of the electrode onto the surface of the jet. Air issuing from the coaxial air cap impinges upon the jet, atomising it, and the water droplets breaking off from the jet retain some of the excess charge. Consequently, the charge on the spray droplets has the opposite polarity to that of the elevated voltage electrode.

The elevated voltage electrode does not touch the water stream and current does not flow directly from this electrode to the droplets. The elevated voltage electrode induces a field which causes charge to flow in a secondary low voltage circuit: firstly, from the earth to the water stream; secondly, from the water stream to the droplets; and, finally, on the droplets through the air to earth.

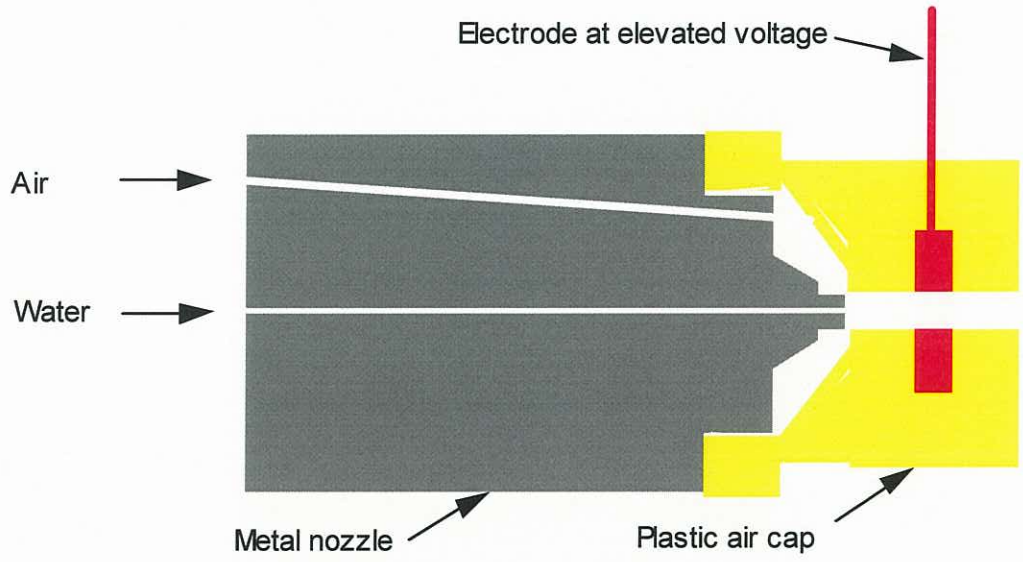

Fig. 3.2 Schematic of the induction-charged air-atomising nozzle (adapted from Cross & Smith 1994)

When properly implemented, taking into account geometrical and hydrodynamic considerations, the design has several attractive features.

a. The elevated voltage electrode is completely embedded within the nozzle.

b. For a relatively moderate applied voltage, a high field gradient can be achieved, limited only by dielectric breakdown of the air.

c. The air flow should maintain the induction electrode completely dry, reducing the possibility of reverse ionisation by corona discharge from droplets on the electrode surface.

3.3 DESCRIPTION OF THE ECWSC RIG

3.3.1 Introduction

The Electrostatically Charged Water Spray Collection (ECWSC) Rig (fig. 3.3) was designed and constructed in order to facilitate the testing of electrostatically charged water spraying devices and the measurement of the following spray parameters.

a. The total current carried by the spray.

b. The spray charge in individual regions of the spray cloud.

Fig. 3.3 The ECWSC Rig

3.3.2 The induction-charged air-atomising nozzle

The induction-charged air-atomising nozzle or other electrostatically charged water spraying device is arranged to spray vertically downwards. For convenience, the complete induction-charged air-atomising nozzle assembly (designed for use with the ECWSDS Rig and, consequently, described in detail below in section 3.4.2) is employed. It is supported from a yoke by a single vertical continuously threaded bar which facilitates the vertical adjustment of its position. The yoke is hung, in turn, from the soffit of the roof slab above the rig by two tubular support members. In order to isolate the induction-charged air-atomising nozzle assembly, the yoke and support members are fabricated from insulating materials.

3.3.3 The spray collector

The spray from the induction-charged air-atomising nozzle or other electrostatically charged water spraying device is retained in a vertical, cylindrical spray vessel or collector as illustrated in figure 3.3 above. The spray collector is connected to earth via a current measuring system (see section 3.3.5 below) but is otherwise electrically isolated. It is 1500 mm high and 650 mm in diameter with planar ends. The upper end incorporates a 220 mm nominal diameter coaxial hole in order to accommodate the induction-charged air-atomising nozzle assembly with sufficient clearance to provide electrical isolation. Two 'portholes' of 180 mm nominal diameter are provided to facilitate access for a Faraday bucket in order to determine spray charge in individual regions of the spray cloud.

In order to ensure discharge of the spray upon contact with the vessel, or with the body of water accumulated therein, the vessel was fabricated from galvanised steel. Its dimensions were largely determined by the need to contain the electrostatically charged spray with minimal loss.

3.3.4 Measurement of pressure and flowrate

3.3.4.1 Water

Water is fed to the induction-charged air-atomising nozzle assembly from the UNSW reticulated water supply via an RMC (Reliance Manufacturing Company) model AC50B pressure reducing value. This provides an outlet pressure that is fully adjustable from zero to the maximum supply pressure of 400 kPa. A line strainer with a monel gauze element is fitted on the inlet side of the valve.

Water flowrates in the range 50 to 800 mL/min are determined using a Platon model NGIB211 flow meter fitted with a precision glass flow tube type GTF2AHS-C that affords a published accuracy of ±10 mL/min. Calibration of the flow meter utilises measured weights of water. Water pressures are measured by a Dwyer Spirahelic pressure gauge model 7114A-

G060. This has a range of 0 to 60 psi (414 kPa) and an accuracy conforming to ASME Grade 3A (0.25% full scale). Calibration of the pressure gauge utilises a dead weight tester.

3.3.4.2 Air

Air is supplied to the induction-charged air-atomising nozzle assembly from the UNSW School of Mining Engineering reticulated compressed air supply via an SMC Pneumatics model AW3000-02B filter/regulator. This provides an outlet pressure that is fully adjustable from zero to the maximum supply pressure of 690 kPa (100 psi).

Air flowrates are measured using one of two flow meters that are arranged for parallel alternative operation.

a. A Platon model GL flow meter fitted with a precision glass flow tube type GTF3AHS-B which has a range of 10 to 100 L/min and which affords a published accuracy of ±1.25 L/min.

b. A Key Instruments model FR4A70BNBN flow meter which has a range of 30 to 280 L/min and which affords a published accuracy of ±8.4 L/min.

Calibration of the flow meter utilises measured weights of compressed air supplied from portable cylinders. Air pressures are measured by a Dwyer Spirahelic pressure gauge model 7114A-G200. This has a range of 0 to 200 psi (1379 kPa) and an accuracy conforming to ASME Grade 3A (0.25% full scale). Calibration of the pressure gauge utilises a dead weight tester.

3.3.5 Measurement of voltage and current

Power to energise the induction-charged air-atomising nozzle at a potential of 0 to ±5000 volts dc is supplied by a Stanford Research Systems model PS350 dc power supply. This is able to provide up to 5000 μA current with a resolution of 1 μA and a voltage resolution of 1 volt.

The measurement of current flowing from the spray to earth was performed by a Keithley model 614 electrometer which has the functionality, on the appropriate range setting, to measure currents of up to 20 μA with a resolution of 1 nA.

Because both the power supply drain current and the spray current exhibited rapid fluctuations, computerised data acquisition was employed in order to characterise them. Both the power supply and the electrometer have an analogue output facility where the output signal (voltage) is proportional to the current being monitored. The range of the analogue outputs is compatible with the input range of standard data acquisition boards.

3.3.5.1 Computerised data acquisition - hardware

Data acquisition is provided via an Apple Macintosh Quadra 840AV personal computer with a National Instruments NB-MIO-16XL-42 data acquisition board installed in No. 4 NuBus slot.

The analogue signals from the power supply and electrometer are connected in parallel mode via a 50-conductor ribbon cable to the data acquisition board. The latter is a multifunction analogue, digital and timing input/output board. It includes a 16-bit analogue to digital converter, 16 multiplexed inputs, two 12-bit digital to analogue converters, 8 digital input/output lines and three 16-bit counters/timers.

The fastest available scanning rate for analogue to digital conversion (using interrupts) is of the order of 5000 samples per channel per second.

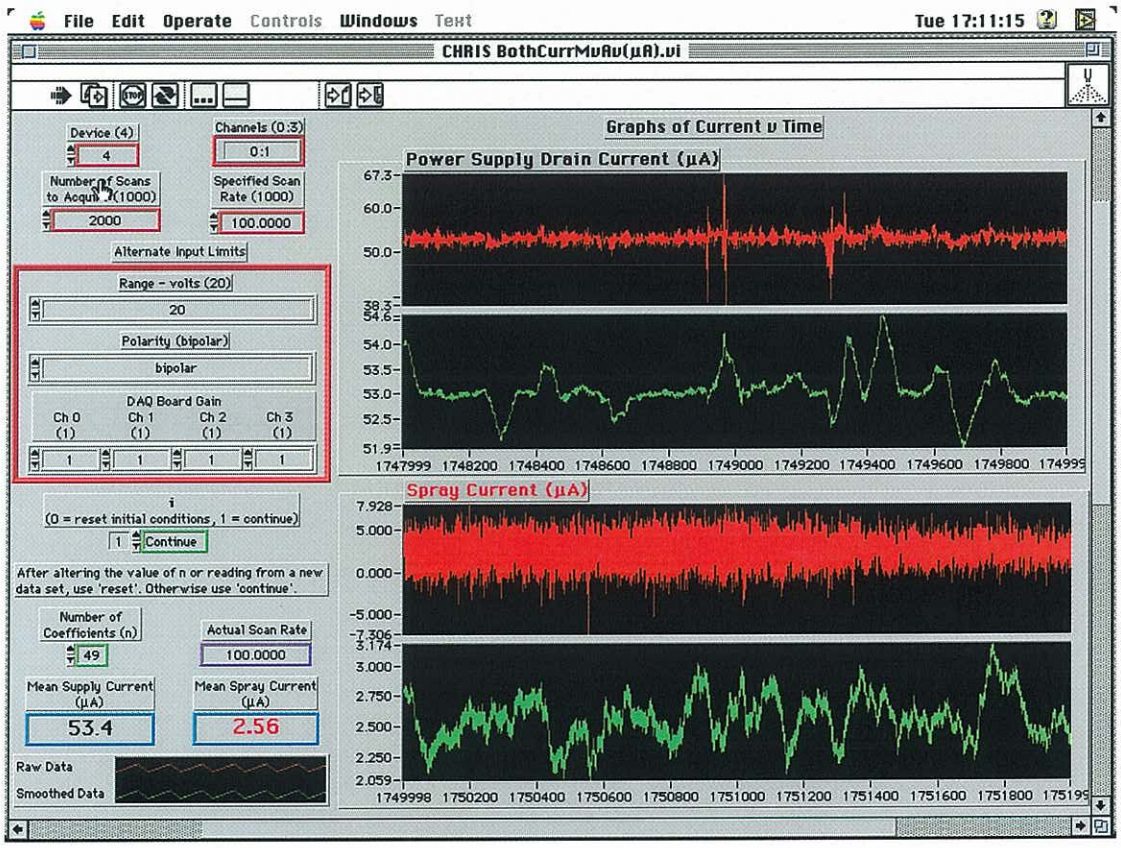

Fig. 3.4 Computerised data acquisition

3.3.5.2 Computerised data acquisition - software

Software comprises National Instruments LabVIEW version 3.0.1 running under Macintosh System Software version Z1-7.5.

LabVIEW software is based on the concept of the virtual instrument, or VI, a software emulation of test equipment that creates, analyses, and displays data much as physical instruments do. It facilitates data capture and analysis without requiring access to dedicated test equipment. It utilises a graphical programming language in which the manipulation of objects replaces the more familiar writing of code. It is used to create applications for data acquisition and management, signal and transient analysis, and process control.

A LabVIEW data acquisition VI was created which 'grabs' a sample of signed 16-bit integer output from the A/D converter for both the 'power supply drain current' and 'spray current' channels. It then plots the 'raw' data from each channel on a waveform chart together with 'smoothed' data from the same channel in the form of a moving mean (see figure 3.4 above). The degree of smoothing, specified by the number of coefficients in the moving mean, may be selected by the user. The VI also calculates and displays the overall mean for each channel.

Input to the VI defines the following parameters. Default values, which may be varied interactively by the user, are given in parentheses.

a. The scan rate at which data is to be acquired, i.e. the number of samples per second per channel (100).

b. The number of scans to acquire (2000).

c. The number of coefficients in the smoothing algorithm (49).

3.4 DESCRIPTION OF THE ECWSDS RIG

3.4.1 Introduction

The Electrostatically Charged Water Spray Dust Suppression (ECWSDS) Rig was specially constructed in order to confirm the efficacy of dust capture by electrostatically charged water spraying, to investigate the effects of the principal design and operational variables on dust suppression efficiency and to determine the enhancement in dust suppression when compared with uncharged sprays.

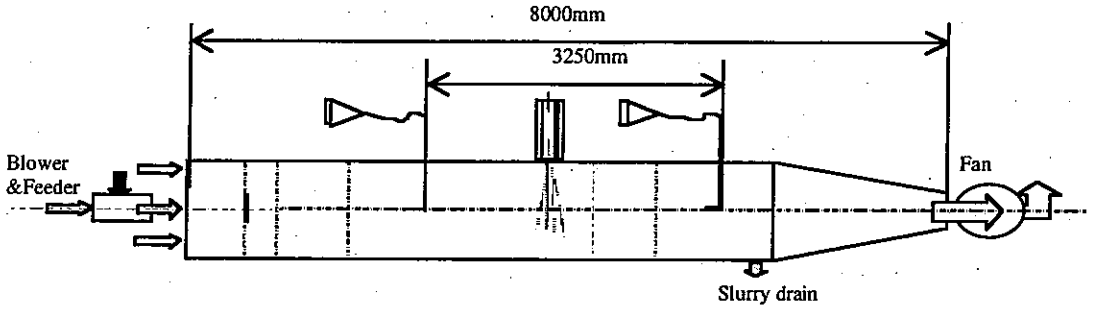

Fig. 3.5 ECWSDS Rig – schematic

The concept of the ECWSDS Rig is illustrated in figure 3.5. Its principal features are as follows.

1. A cylindrical/tapering body fabricated from galvanised steel and comprising an eight metre long, subhorizontal, cylindrical 'wind tunnel', generally of 650 mm diameter.
2. A dust injector (fig. 3.6 below) that introduces coal dust into the body of the rig.
3. An exhaust fan (fig. 3.7 below) that maintains a negative gauge pressure and, hence, a flow of air through the body of the rig, simulating the flow of ventilation air.
4. The induction-charged air-atomising nozzle assembly (fig. 3.9 below) mounted in a spray tower (fig. 3.8 below) located on the body of the rig and orientated to spray vertically downwards.
5. Two dust sampling tubes located 'upstream' and 'downstream' of the spray tower in regions free from water spray.

Each dust sampling tube may be removed from its port and replaced by an air velocity measuring device, a TSI VelociCheck hot wire anemometer (sec 3.5.1.2) fitted with a telescopic probe such that the measuring head can traverse the full diameter of the 'wind tunnel'.

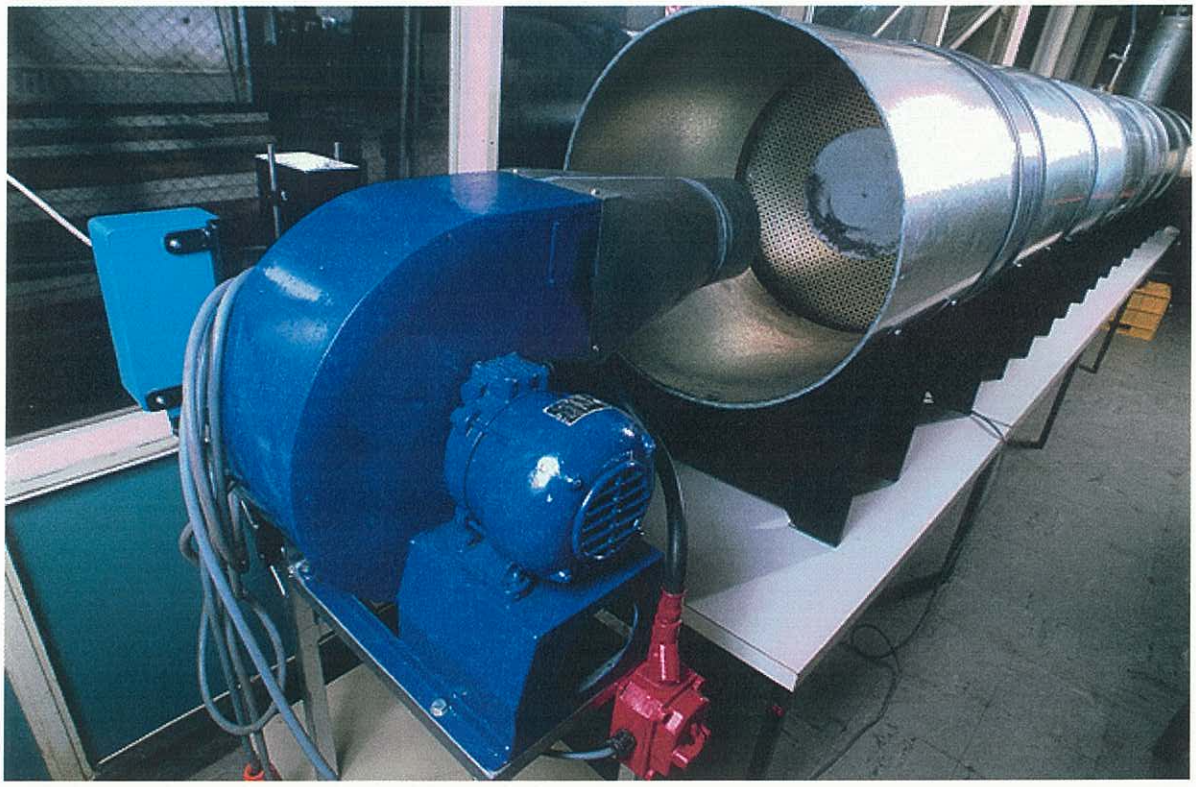

Fig. 3.6 ECWSDS Rig – from dust injector end

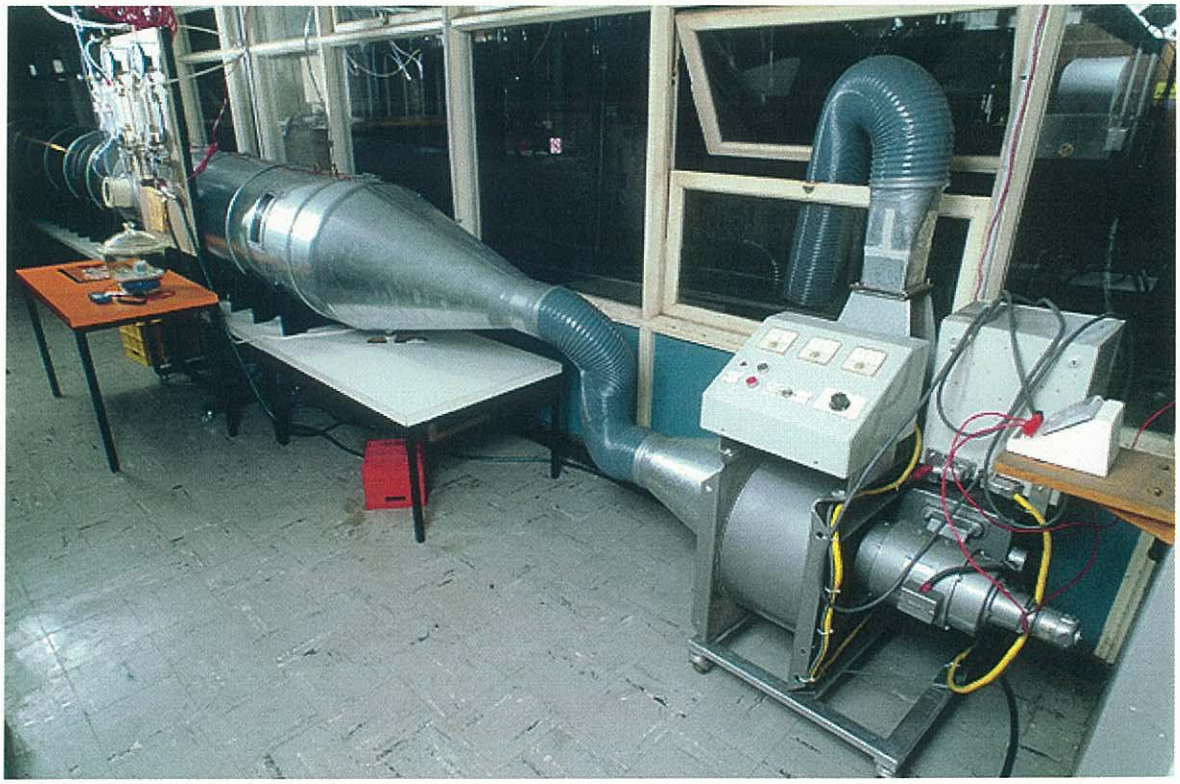

Fig. 3.7 ECWSDS Rig – from exhaust fan end

3.4.1.1 The 'wind tunnel'

The body of the ECWSDS Rig, the 'wind tunnel', is fitted with a series of internal baffles in order to ensure a uniform air velocity and homogeneous dust concentration in the 'test section'. This is defined as extending 3250 mm from the 'upstream' dust sampling location to the 'downstream' dust sampling location (fig. 3.5).

Additional ports are provided within the 'test section' in order to facilitate the determination of variations in air velocity in both the transverse and longitudinal directions and the undertaking of dust sampling surveys in order to verify the homogeneity of the dust concentration.

3.4.1.2 The dust injector

The dust injector is shown in figure 3.6 above. It comprises a hopper from which the coal dust flows onto a vibrating feeder and then into the fan which blows it into the body of the Rig via a 180 mm nominal diameter injection tube. The fan speed is fixed but the dust injection rate can be varied by altering the amplitude of vibration of the feeder.

3.4.1.3 The exhaust fan

The exhaust fan, shown in figure 3.7 above, is thyristor controlled such that the air velocity through the 'test section' of the rig can be varied between 0 and 1.25 metres per second.

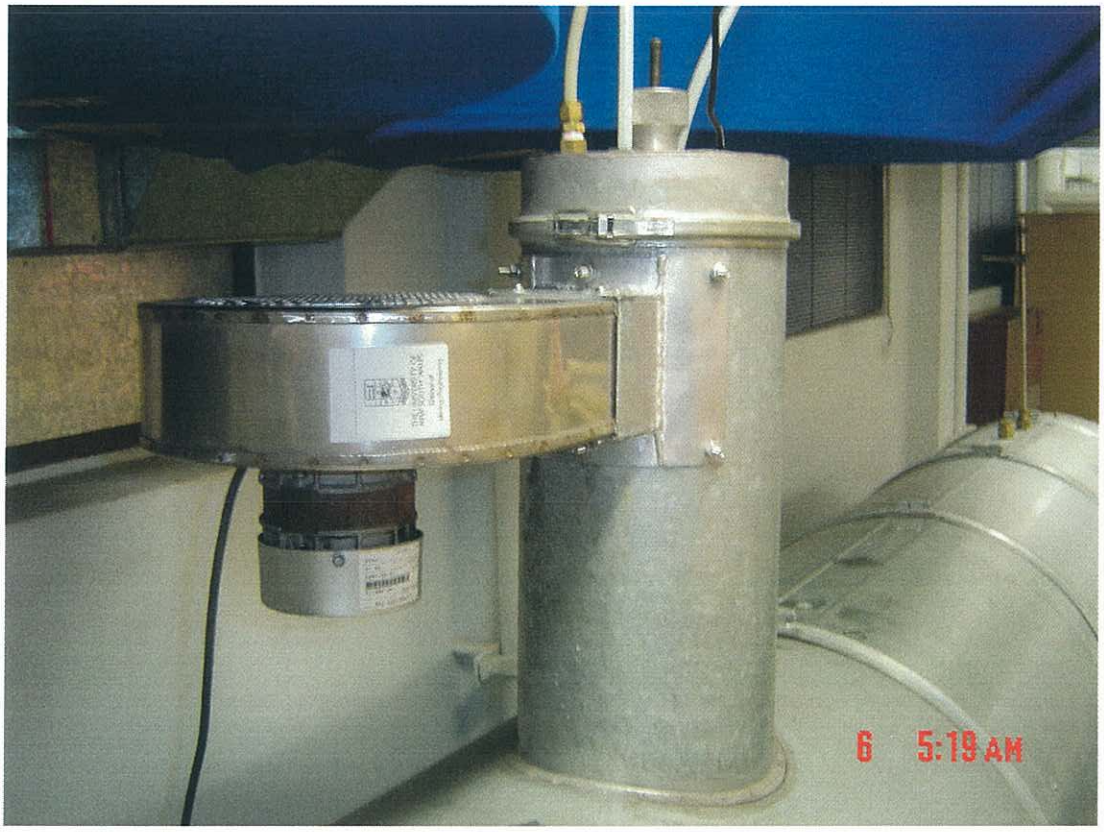

Fig. 3.8 The 'spray tower'

3.4.1.4 The spray tower

A cylindrical 'spray tower', shown in figure 3.8 above, is mounted on the body of the ECWSDS Rig in the centre of the 'test section' in order to accommodate the induction-charged air-atomising nozzle assembly or other electrostatically charged water spraying device.

The 450 mm long spray tower is of 200 mm nominal diameter and is closed by a planar end cap. The induction-charged air-atomising nozzle assembly is designed to be a flush fit within the tower. A 'purging air fan' is mounted on the tower in order to ensure that a supply of clean, dry air passes through the labyrinth in the induction charging electrode assembly (sec. 3.4.2). The fan is a Markair Components 'Bingo Blower' rated at 250 cfm (118 L/s).

A 150 mm nominal diameter opening 'porthole' is provided in the main body of the ECWSDS Rig on the same transverse plane as the spray tower in order to facilitate access for a Faraday bucket in order to determine spray charge in individual regions of the spray cloud.

3.4.2 The induction-charged air-atomising nozzle assembly

The induction-charged air-atomising nozzle assembly is shown in figure 3.9.

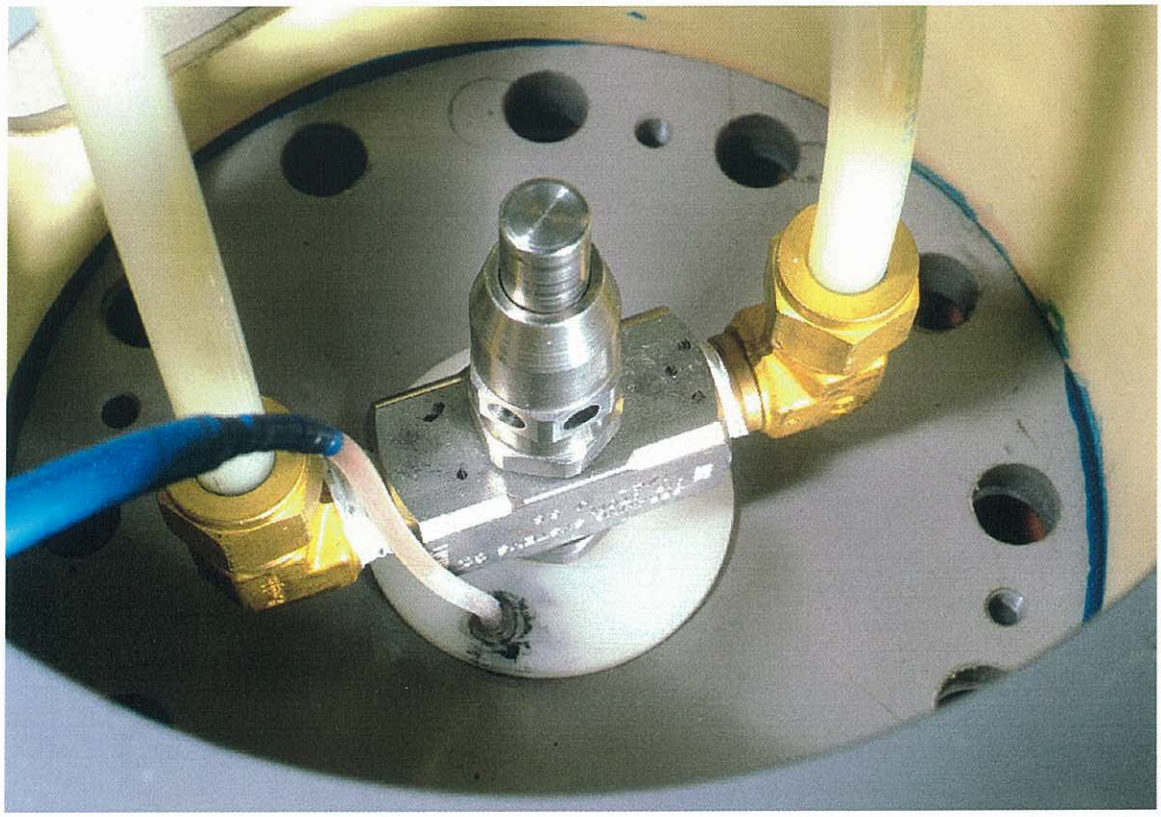

Fig. 3.9 Induction-charged air-atomising nozzle assembly

The induction-charged air-atomising nozzle assembly was mounted in the 'spray tower'. It was identical with that employed in connection with the programme of testing using the ECWSC Rig (sections 3.2 & 3.3). It was not practicable, however, to utilise an air gap to electrically isolate the assembly as had been done in the case of the ECWSC Rig. Consequently, elaborate means had to be employed to prevent current short circuiting from the elevated voltage induction charging electrode to the 'spray tower' which formed an integral part of the body of the ECWSDS Rig and was maintained at earth potential. The problem was that the elevated voltage electrode needed to be supported within the 'spray tower' in an environment of water spray and wet coal dust. Consequently, it was necessary to prevent the support from acting as a wet, dusty, conducting path to earth and shorting out the power supply.

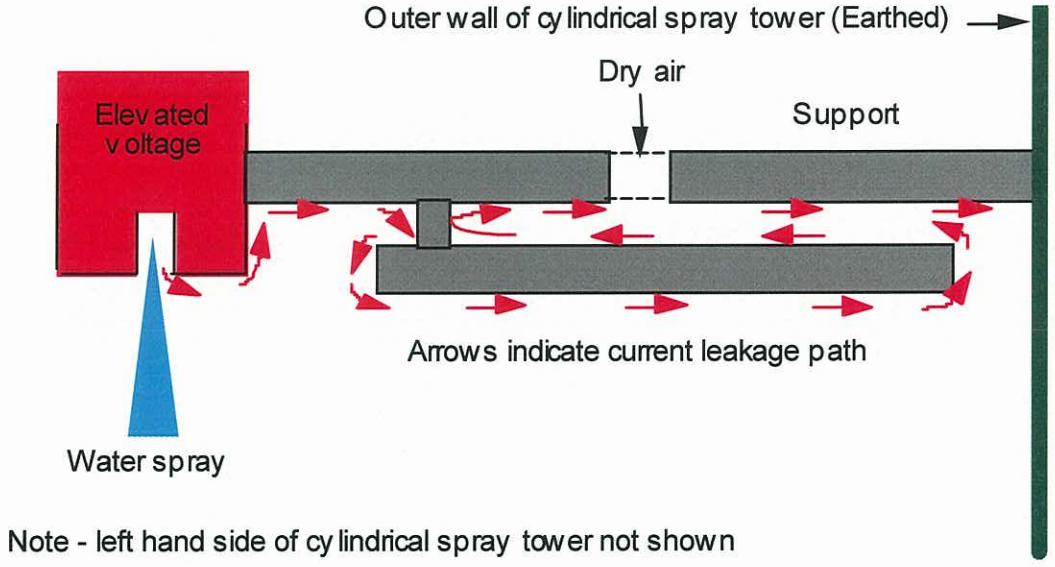

Fig. 3.10 Elimination of current leakage between elevated voltage electrode and ECWSDS Rig (adapted from Cross & Smith 1994)

The means used to achieve this, as illustrated in figure 3.10, were to force leakage current from the elevated voltage electrode to flow around a labyrinth, into which clean dry air was blown by the purging air blower, in order to reach the earthed wall of the 'spray tower'. The path that the current was constrained to follow is shown by arrows in the figure. The labyrinth utilised materials such as Teflon, silicon rubber and anti-tracking lacquer in order to obviate current tracking. The leakage current was reduced by these means to an acceptable level.

The arrangements for the supply of air, water and electrical power to the induction-charged air-atomising nozzle assembly were identical with those described in sections 3.3.4 and 3.3.5 in connection with its employment with the ECWSC Rig.

3.5 DETERMINATION OF DUST SUPPRESSION EFFICIENCY

Gravimetric sampling was employed to confirm the efficacy of dust capture by electrostatically charged water sprays, to investigate the effects of the principal design and operational variables on dust suppression efficiency and to determine the enhancement in dust suppression when compared with uncharged sprays.

At the commencement of the programme of laboratory testing, it was envisaged that only one type of coal dust would be employed and that the particle size distribution of the unsuppressed dust would be determined after each test in order to 'separate' the capture efficiency of the inspirable and respirable fractions.

7027 stnd leu341x

Upper	in	Lower	Under	Upper	in	Lower	Under	Upper	in	Lower	Under	Span 3.36
				124	0.8	101	97.8	11.6	6.7	9.48	38.5	
				101	1.1	83.3	96.7	9.48	6.0	7.78	32.5	D[4,3] 21.53µm
				83.3	1.6	68.3	95.1	7.78	5.4	6.39	27.0	
				68.3	2.3	56.1	92.8	6.39	4.7	5.24	22.4	
600	0.0	492	100	56.1	3.2	46.0	89.6	5.24	4.0	4.30	18.4	D[3,2] 6.25µm
492	0.0	404	100	46.0	4.2	37.8	85.5	4.30	3.4	3.53	15.0	
404	0.0	332	100	37.8	5.3	31.0	80.2	3.53	3.1	2.90	11.9	
332	0.1	272	99.9	31.0	6.2	25.5	74.0	2.90	2.7	2.38	9.2	D[v,0.9] 47.00µm
272	0.1	224	99.7	25.5	7.0	20.9	67.0	2.38	2.4	1.95	6.8	
224	0.2	183	99.5	20.9	7.3	17.1	59.7	1.95	2.0	1.60	4.8	
183	0.3	151	99.2	17.1	7.4	14.1	52.2	1.60	2.1	1.32	2.7	D[v,0.1] 2.53µm
151	0.5	124	98.6	14.1	7.1	11.6	45.1	1.32	2.7	0.50	0.0	

Source = :Sample	Beam length = 2.2 mm	Model indp	D[v,0.5] 13.24µm
	Residual = 0.295 %		
Focal length = 300 mm	Obscuration = 0.2307	Volume Conc. = 0.0235%	
Presentation = stnd	Volume distribution	Sp.S.A 0.9607 m²/cc.	

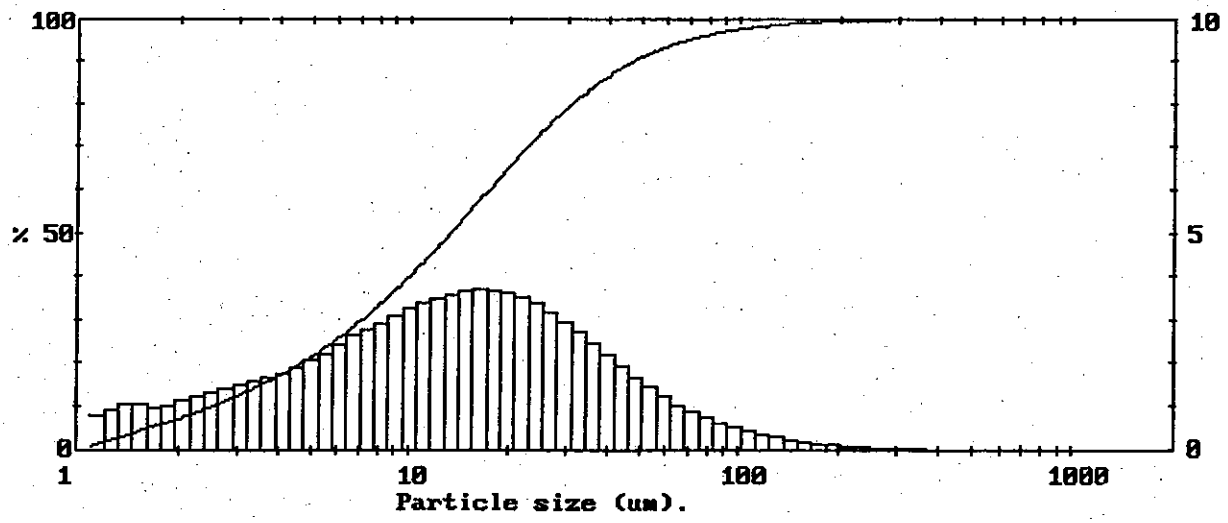

Fig. 3.11 Type 1 (inspirable) dust - particle size distribution

The particle sizing procedure, however, proved to be too time consuming and cumbersome to be employed on such a basis. Consequently, it was concluded that the issue of the suppression efficiency of the inspirable and respirable dust fractions would be addressed by undertaking separate testing programmes.

Finely milled coal dispersed in the air was used to simulate airborne coal dust. Two grades were employed: Type 1, approximately analogous to inspirable dust and Type 2, very finely ground to simulate respirable dust. The particle size distribution of the Type 1 coal dust is given in figure 3.11 above from which it will be seen that the mean particle diameter D[4,3] was of the order of 21 μm and that almost 98% of the material was less than 100 μm in diameter. The particle size distribution of the Type 2 (respirable) coal dust is given in figure 3.12 from which it will be seen that the median particle diameter was 3 μm and that 100% of the material was less than 8 μm in diameter.

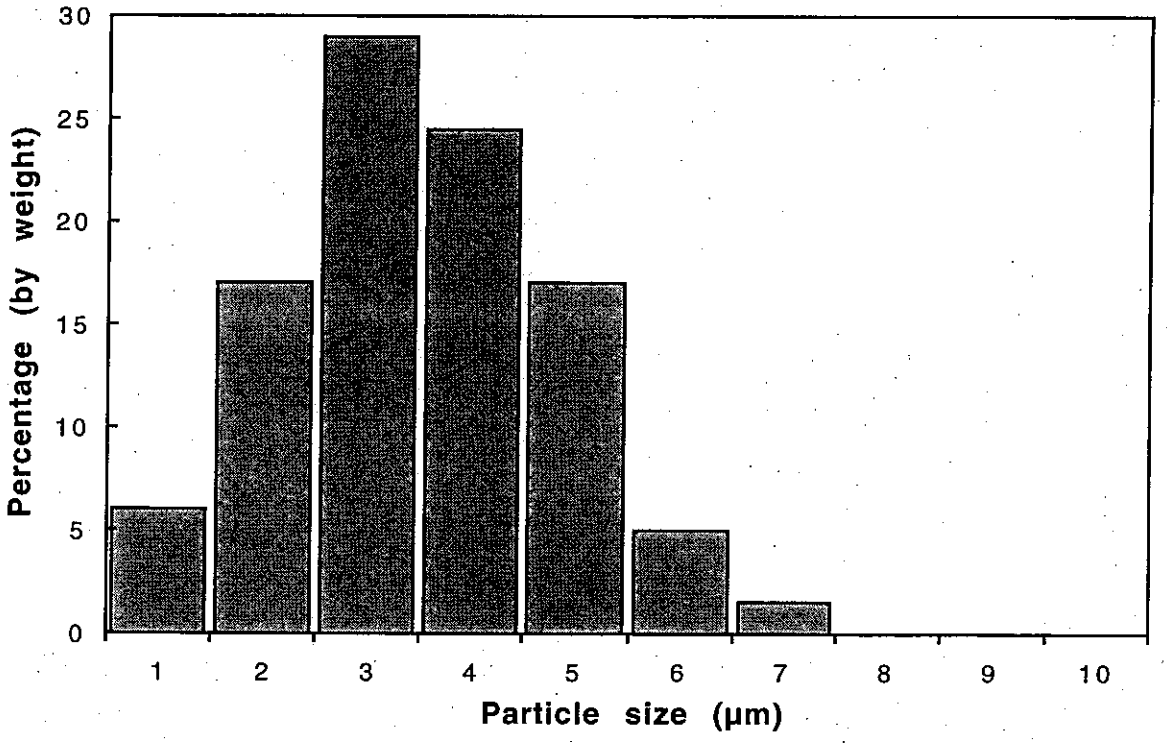

Fig. 3.12 Type 2 (respirable) dust - particle size distribution

The dust sampling arrangement is shown in figure 3.13 below. A vacuum pump draws dust laden air from the 'test section' of the ECWSDS Rig into sampling tubes located 'upstream' and 'downstream' of the water spray. The air passes through filter membranes, which retain the coal dust, and then via flow meters to the pump. The main components of the air sampling arrangement are described in outline below.

- Two 'L'-shaped sampling tubes each fabricated from stainless steel of 9.4 mm bore.

- Two filter membranes (sec. 3.5.1.3), each retained in a Pall Corporation 47 mm In-line Polycarbonate Filter Holder between a polyphenylsulfone support screen and a silicone O–ring (fig. 3.15).
- A pair of Influx Type SSS flow meters, each fitted with a precision glass flow tube Type S of range 0.6 to 5.0 mL/min which conforms to VDI/VDE class 2.5, i.e. affords a stated accuracy of 1.875% of reading plus 0.626% of full scale. Calibration of the flow meters utilised measured weights of compressed air supplied from portable cylinders.
- A Dynavac Model OD1/2 vacuum pump. This is an oil free diaphragm device that can generate a maximum continuous vacuum of -71 kPa and achieve a flow rate of 13 L/min against a vacuum of -25 kPa.

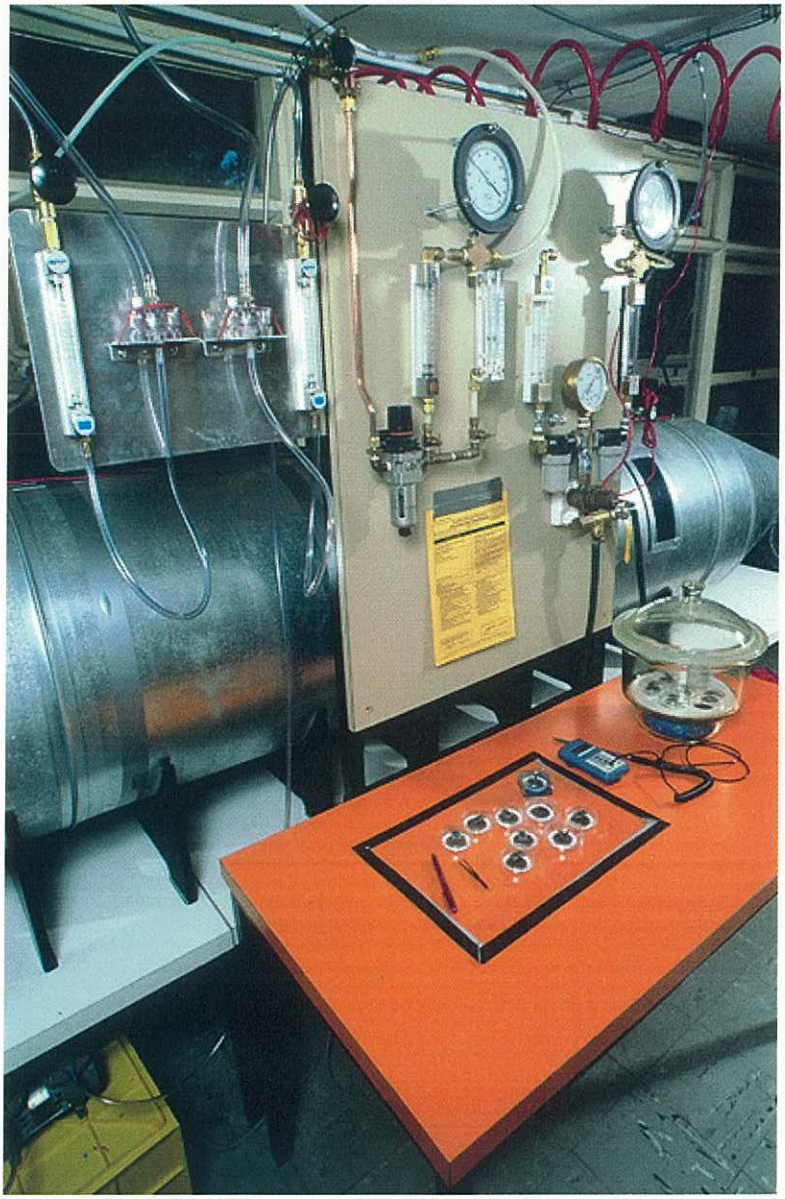

Fig. 3.13 Dust sampling arrangement

3.5.1 Determination of dust concentration by gravimetric sampling

The gravimetric sampling protocol followed the relevant standards, Australian Standard AS 2985–1987 *Workplace atmospheres–Method for sampling and gravimetric determination of respirable dust* and AS 3640–1989 *Workplace atmospheres–Method for sampling and gravimetric determination of inspirable dust*.

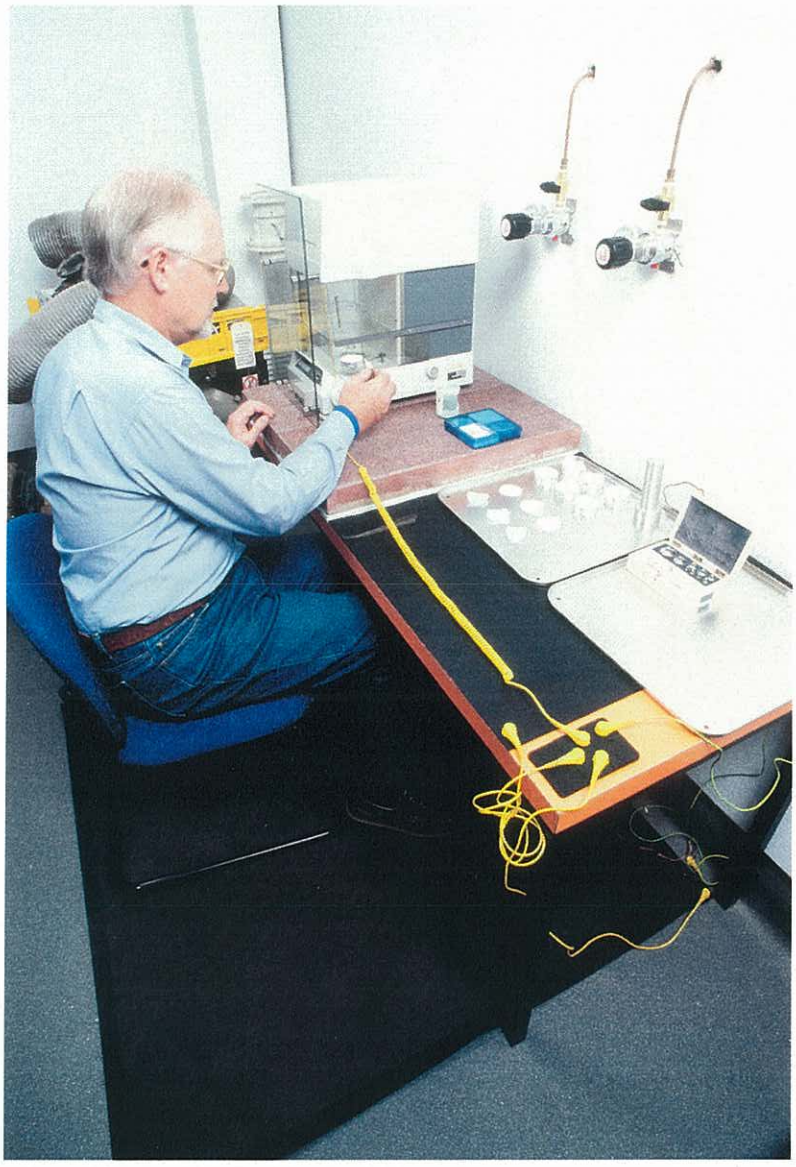

Fig. 3.14 Weighing filter membrane and dust load

Essentially, a known volume of dusty air was drawn from the 'upstream' and 'downstream' sampling locations in the 'test section' of the ECWSDS Rig through pre-weighed filter membranes and the weights of dust determined from the increases in weight of the membranes. The dust concentrations could then be obtained from the quotients of the weights

of dust and the volume of air. Dust suppression efficiency could then be determined by comparing the 'upstream' and 'downstream' dust concentrations.

Some of the more important issues that had to be addressed in order to ensure accuracy in the determination of dust concentration are outlined below.

3.5.1.1 Accuracy in weighing coal dust

AS 2985–1987 and AS 3640–1989 both specify that the balance used to weight the filter membrane and dust load should have an accuracy of ±20 μg. In practice, a Sartorius Model 2405 Microbalance (fig. 3.14 above) with a resolution of ±1 μg was available to the project. The balance was calibrated to an accuracy of ±10 μg.

3.5.1.2 Isokinetic sampling

Dust in the 'test section' was sampled via the 'L'-shaped stainless steel tubes which were orientated in such a way that one arm was parallel to the longitudinal axis of the ECWSDS Rig. In order to ensure accuracy, sampling was isokinetic, i.e. the velocity of air in the sampling tube was arranged to be the same as the velocity of air in the 'test section' at the sampling point.

The latter was determined before each series of tests using a TSI VelociCheck Model 8330-M-GB Portable Air Velocity Meter. This is a hot wire anemometer having a range of 0 to 20 m/s, a resolution of 0.01 m/s, a stated accuracy of ±5% of reading or ±0.025 m/s, whichever is greater, and a calibration traceable to the National Institute of Standards and Technology (NIST). The diameter of the sampling tube was constrained by the practical requirement of ensuring a dust load and sampling time that could both be determined with a high degree of accuracy (sec. 3.5.1.6).

3.5.1.3 Filter membrane material

Ideally, the filter membrane material should be insensitive to changes in environmental factors such as temperature and humidity. In addition, it should be robust and readily handled, not be liable to material loss and be unaffected by electrostatic charge. An extensive series of tests was undertaken in order to determine the most suitable filter membrane. The materials tested are listed below in table 3.1.

Further information on the filter membrane materials is given in SKC (2001) and Millipore (2001). None of the materials tested was ideal. However, the properties of the Type G filter membrane, Millipore Fluoropore FHLP 047 00 (polytetrafluoroethylene bonded to poly-ethylene), were such that it most closely met the requirements and was selected for use.

Table 3.1 Filter membrane materials for gravimetric sampling

Type	*Supplier & reference number*	*Proprietary name*	*Material*	*Pore size*
				µg
A	SKC 225-504		Mixed cellulose acetate and nitrate	0.80
B	Millipore AAWG 047 00	MF- Millipore	Mixed cellulose acetate and nitrate	0.80
C	Millipore AAWP 047 00	MF- Millipore	Mixed cellulose acetate and nitrate	0.80
D	Millipore HAWG 047 00	MF- Millipore	Mixed cellulose acetate and nitrate	0.45
E	Millipore HTTP 047 00	Isopore	Polycarbonate	0.40
F	Millipore HVLP 047 00	Durapore	Hydrophilic polyvinylidene fluoride	0.45
G	Millipore FHLP 047 00	Fluoropore	Polytetrafluoroethylene bonded to polyethylene	0.50
H	Millipore AP15 047 00	AP15	Borosilicate microfibre glass	
I	Millipore FHLC 047 00	LCR Membrane	Hydrophilized polytetrafluoroethylene	0.50
J	Millipore LSWP 047 00	Mitex	Polytetrafluoroethylene	5.00
K	Millipore PVC0 847 00	PVC Membrane	Polyvinylchloride	0.80

3.5.1.4 Filter membrane arrangement

Gravimetric analysis often utilises a double arrangement that employs two pre-weighed filter membranes, the sample filter and the control filter, placed one on top of the other in a single filter holder. During filtration, the dust should be retained entirely by the upper (sample) filter. However, both filters should be subjected to identical alterations in tare weight as a result of moisture loss or gain or other environmental factors. Any change in weight of the lower (control) filter could then applied as a correction to the weight of the coal dust.

A series of tests was undertaken to determine the efficacy of this technique. Unfortunately, it proved to be less accurate than the simple, single filter membrane arrangement shown in figure 3.15 below. The reason for this is believed to be a tendency for the sample filter to shed from itself material that is then collected by the control filter. Consequently, a single filter membrane arrangement was adopted. Accuracy in the determination of the coal dust weight was maintained by closely controlling the environment and adopting a rigorous conditioning protocol (sec. 3.5.1.7).

3.5.1.5 Electrostatic charge on milled coal (coal dust)

As an electrostatic charge on the finely milled coal (coal dust) would adversely affect the weighing process, a series of tests was undertaken in order to determine whether the milled coal was charged or neutral. The tests utilised an electrometer and Faraday cup. Two electrometers were available to the project, a Keithley Model 602 and a Model 614.

The charge-to-mass ratio of the milled coal, when sampled directly from a storage container, was low. However, the charge-to-mass ratio of samples of milled coal taken from the 'downstream' sampling location was very high, too high to determine using the available electrometers. It was conjectured that the increase in electrostatic charge was caused by the transfer of electrostatic charge from the water droplets to the dust and, consequently, to the filter membrane.

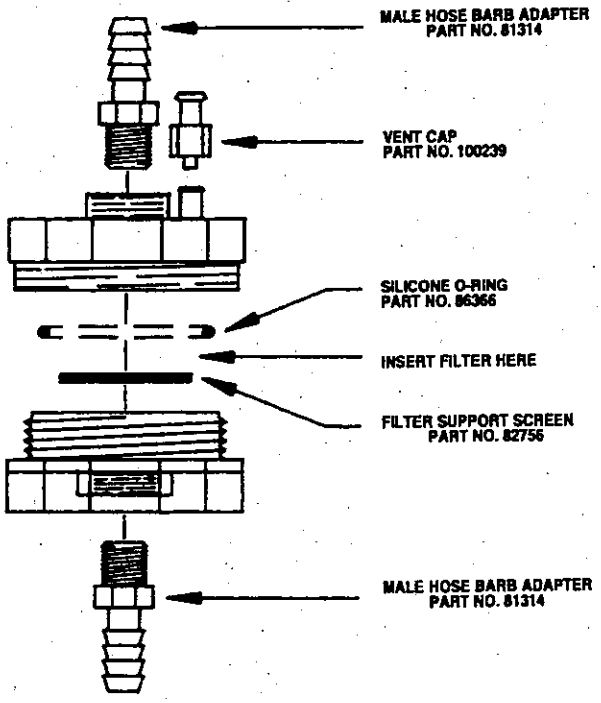

Fig. 3.15 Installation of single filter in Pall Corporation 47 mm in-line filter holder

The high electrostatic charge interfered with the operation of the Microbalance despite the use of a static eliminator, an alpha particle source ionising unit (Polonium 210 radioisotope of 2×10^5 Bq activity). Consequently, a technique was adopted where the membrane filter plus dust load was weighed in a pre-weighed circular aluminium 'pie dish' (visible in figure 3.14) which shielded the Microbalance from the effect of the electrostatic charge. The 'pie dishes' were made from 20 µm thick aluminium foil. Their base diameter was 48.5 mm to accommodate the 47 mm nominal diameter filter membranes and their height was 15 mm.

3.5.1.6 Maximum coal dust load on filter membrane

A series of tests was undertaken to determine the maximum quantity of coal dust that could be collected without overloading the filter membrane. It was concluded that a maximum weight of the order of 30 mg was generally appropriate. A greater quantity of dust resulted in handling difficulties and the attendant possibility of dust spillage, particularly while removing the membrane from the filter holder and getting it into and out of the 'pie dish' during the weighing procedure. As the Microbalance had been calibrated to an accuracy of ±10 μg (sec. 3.5.1.1), an accuracy of ±0.03% in the determination of the weight of coal dust was the best that was theoretically achievable.

3.5.1.7 Conditioning of filter membranes and dust load

In order to allow the filter membranes to achieve equilibrium with the atmosphere of the balance room, each filter was conditioned on an earthing plate for a minimum of 24 hours prior to its being weighed. The weighing was then repeated the following day. Provided that the readings agreed to within 10 μg the filters were used for dust sampling. Otherwise, the process of conditioning and reweighing was continued until agreement was achieved.

A similar conditioning procedure was undertaken with dust laden filters the only difference being that the acceptance criterion was increased to 20 μg.

3.5.2 Testing procedure

The remainder of this section briefly outlines the procedure employed to determine the concentration of airborne coal dust using the ECWSDS Rig.

Prior to each series of tests, the following relationships were determined.

- Between the exhaust fan motor speed setting and the air velocity through ECWSDS Rig
- Between the dust injector setting and the approximate dust concentration in the ECWSDS Rig at the 'upstream' sampling location.

Prior to each test, the values of the following parameters were set.

- The exhaust fan motor speed setting
- The polarity and voltage of the power supply output to the induction charging electrode
- The atomising air pressure
- The water flowrate to the induction-charged air-atomising nozzle
- The dust injector setting
- The air flowrate through the 'test section' at the dust sampling locations

Subsequently, the hopper on the dust injector (sec. 3.4.1.2) was filled with coal dust, a pre-weighed filter membrane (sec. 3.5.1.3) was installed in each filter holder and the following items turned on.

- The purging air blower
- The exhaust fan
- The power supply
- The electrometer, in order to measure the current flowing from the water spray to earth
- The computer and data acquisition programme, in order to record the mean spray current and the mean power supply drain current
- The air supply to the induction-charged air-atomising nozzle
- The water supply to the induction-charged air-atomising nozzle
- The dust injector

The vacuum pump that drew the air through the dust sampling arrangement was then run for a predetermined time as measured by an electronic count down timer. During the run, the values of the following parameters were monitored and recorded.

- Both the instantaneous and mean spray current
- Both the instantaneous and mean power supply drain current

Upon completion of the test, the dust laden filter membranes were carefully removed from the filter holder and subsequently conditioned (sec. 3.5.1.7) before being weighed. The dust concentrations and suppression efficiency were then calculated.

4 DEVELOPMENT OF INDUCTION CHARGING THEORY

4.1 INTRODUCTION

Because of the complexity of the induction charging / air atomisation process and the large number of parameters which could potentially effect its efficiency, it was considered essential to have a rigorous theory with which to guide the laboratory investigations and design process.

However, following an extensive review of the literature, existing theories for the induction charging and air atomisation of a liquid jet were found to be inadequate and a new theory was developed, based upon the work of Artana, Bassani and Scaricabarozzi (1992).

Figure 4.1 delineates the region of the induction-charged air-atomising nozzle, illustrated in figures 3.1 and 3.2, which was modelled for the development of the new theory.

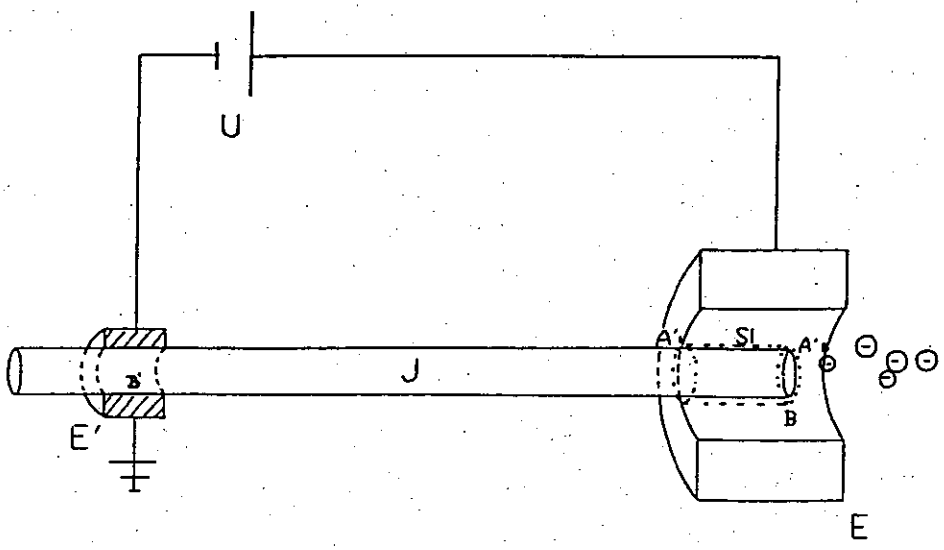

Fig. 4.1 Scheme of the induction charging process
(after Artana, Bassani and Scaricabarozzi 1992)

In developing their theory, Artana *et al* considered that three of the factors to be taken into account were as follows.

a. Capacitance between the charged electrode E and the segment of the liquid jet J contained within the electrode.

b. Resistance of the liquid jet between the outlet of E', the liquid nozzle, and B, the point of jet break up.

c. That which they termed a 'liquid capacitor' between the outlet of the liquid nozzle and the point of jet break up.

However, it is considered that (c) has no physical reality. The liquid jet is at earth potential and, consequently, there can be no capacitance between the jet and earth. This view is shared by others; see, for example, Atten and Oliveri (1992).

The new theory was derived using two independent methods: an equivalent electric circuit method presented in section 4.3 and a method based upon Maxwell's equations of electro-magnetism as set out in section 4.4. The equivalence of the two theoretical models was also demonstrated (sec. 4.6).

4.2 SYMBOLS AND DEFINITIONS

In the analyses set out below, the symbols are assigned the following meanings and units.

A_a cross sectional area of the air annulus, m^2

A_l cross sectional area of the liquid jet, m^2

C capacitance of the combination of cylindrical electrode and liquid jet, F

C_l capacitance per unit length of the cylinder-jet combination, F / m

D diameter of droplet, m

$\mathbf{D}$ electric displacement vector

D_{32} Sauter mean diameter of droplet, μm

d liquid jet diameter, m

E_c corona starting field strength, V/m

E_j radial electric field strength on the surface of the jet, V/m

f_r roughness factor

$\mathbf{H}$ magnetic intensity

i electric current, A

$\mathbf{J}$ current density vector, A/m^2

J_f free current density, A/m^2

L liquid jet break up length, m

L_c length of cylindrical electrode, m

L_j unbroken length of liquid jet inside the cylindrical electrode, m

L' length of liquid jet from the nozzle exit point to the electrode entrance point, m

$\mathbf{M}$ magnetisation

$\dot{m}_a$ mass flow rate of air, kg/s

$\dot{m}_l$ mass flow rate of the liquid jet, kg/s

m_t mass of charged liquid jet or spray, kg

p_j circumference of the liquid jet, m

Q_a volume flow rate of air, m^3 / s

Q_l volume flow rate of liquid jet, m^3 / s

q charge on liquid jet, C

q_d droplet charge, C

q_{sc} specific charge of liquid or charge per unit volume, C / m^3

R_l resistance of liquid jet, Ω

r_c radius of cylindrical electrode, m

r_d droplet radius, m

r_j radius of liquid jet, m

S_0 total surface area of formed droplets or spray, m^2

t charging time, s

V applied voltage, V

V_0 corona starting voltage, V

V_b liquid volume of charged jet, m^3

V_l velocity of the liquid jet issuing from the nozzle, m/s

v the velocity of the tip of the liquid jet or the droplet velocity, m/s

v_{rel} relative air velocity, m/s

α interaction coefficient of air and jet

β_0 charge to mass ratio of spray, C / kg

ε_0 permittivity of air, F/m

ε_r dielectric constant of droplet or particle

ρ_a air density, kg / m^3

ρ_f free charge density, C / m^3

ρ_l liquid density, kg / m^3

σ electrical conductivity of the liquid, S / m

σ_l liquid surface tension, kg / s^2

τ charge transfer time constant or charge relaxation time, s

τ_c characteristic time of electric circuit, s

δ_a relative density of air

μ_l liquid dynamic viscosity, $kg.s/m^2$

4.3 EQUIVALENT ELECTRIC CIRCUIT METHOD

4.3.1 General mathematical model

The process of induction charging of the liquid jet may be represented by an equivalent electric circuit as set out in figure 4.2.

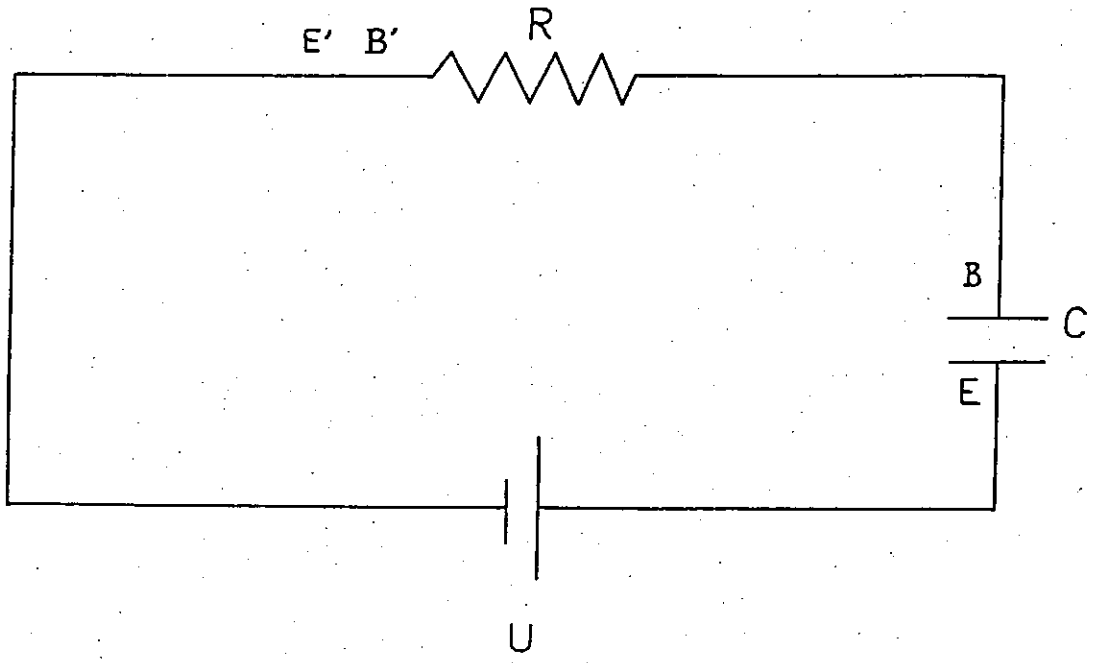

Fig. 4.2 Equivalent electric circuit used to model the induction charging process

The symbols in figures 4.1 and 4.2 are assigned the following meanings.

B jet disintegration point

B' inlet of the earthed electrode

C capacitor formed by the combination of cylindrical electrode and liquid jet

E charged cylindrical electrode

E' earthed electrode (liquid nozzle)

R liquid jet resistor

U dc voltage source

The equivalent electric circuit differs from that postulated by Artana *et al* in that it does not have a capacitor in parallel with the resistor R (sec. 4.1)

The capacitance of the combination of charged cylindrical electrode and liquid jet within the electrode can be shown to be approximated by

$$C = C_l L_j = \frac{2\pi\varepsilon_0}{\ln(r_c / r_j)} L_j \quad \text{..... (4.1)}$$

The resistance R_l of the liquid jet between the earthed electrode E' and the jet disintegration point B may be expressed by

$$R_l = \frac{L}{\sigma A_l} \quad \text{..... (4.2)}$$

where L is the length of the liquid jet between E' and B, i.e. the jet break up length, which is a function of both liquid jet velocity and atomising air velocity. The charging time t is given by

$$t = \frac{L_j}{v}, \quad 0 < L_j < L_c \quad \text{..... (4.3)}$$

Because the jet charging process is an unsteady state, the equation for the induction charging process is written in accordance with Kirchhoff's Laws for the unsteady state as follows.

$$V = iR_l + \frac{q}{C}$$

Substituting

$$i = \frac{dq}{dt}$$

gives

$$V = \frac{dq}{dt} R_l + \frac{q}{C} \quad \text{..... (4.4)}$$

Equation (4.4) is the mathematical representation of the charging rate of a liquid jet based upon the equivalent electric circuit. The form of the equation is a first order differential equation with constant coefficients. The general solution, obtained by standard methods, is

$$q = c_1 e^{-t/RC} + VC \quad \text{..... (4.5)}$$

where c_1 is a constant.

4.3.2 Charge on liquid jet

The charge on the liquid jet is given by a particular solution of the mathematical model that may be obtained by substituting the initial condition $q = 0$ at $t = 0$ into the general solution. Making the substitution in equation (4.5) we obtain

$$q = VC(1 - \exp(-t / R_l C)) \quad \text{..... (4.6)}$$

where $\tau_c = R_l C$ is the characteristic time for the equivalent electrical circuit.

Equation (4.6) is valid for $L_j > 0$ where L_j can be expressed by

$$L_j = L - L' \quad \text{..... (4.7)}$$

In equation (4.7), L is the jet break up length, i.e. the total length of the liquid jet from the nozzle exit point to the jet disintegration point, while L' is the distance between the nozzle exit point and the electrode entrance point.

If $L_j \leq 0$ the jet breaks up at or before the electrode entrance point and, hence, no charging occurs. Conversely, should the jet disintegration point be downstream of the electrode, the expression for length L would become

$$L = L' + L_c \quad \text{..... (4.8)}$$

where L_c is the length of the cylindrical electrode.

4.3.3 Specific charge of liquid jet and charge to mass ratio

By dividing equation (4.6) by the volume of the liquid jet $V_b = Q_l t = Q_l L_j / v$, we derive an expression for q_{sc}, the specific charge of the liquid jet,

$$q_{sc} = C_l V \cdot \frac{v}{Q_l}(1 - \exp(-t / R_l C)) \quad \text{..... (4.9)}$$

Alternatively, by dividing equation (4.9) by the density of the jet liquid ρ_l, we obtain an expression for β_0, the charge to mass ratio of the spray,

$$\beta_0 = q / m_l = \frac{C_l V}{\rho_l Q_l} \cdot v \cdot (1 - \exp(-t / R_l C)) \quad \text{..... (4.10)}$$

Substituting for C_l gives us

$$\beta_0 = q / m_l = \frac{2\pi\varepsilon_0 V}{\rho_l Q_l \ln(r_c / r_j)} \cdot v \cdot (1 - \exp(-t / R_l C)) \quad \text{..... (4.11)}$$

4.4 INDUCTION CHARGING MODEL BASED UPON MAXWELL'S EQUATIONS

4.4.1 General mathematical model

The scheme of the induction charging process for modelling by Maxwell's equations of electromagnetism is shown in figure 4.1 above. The broken line in the figure represents the integration surface within the charged cylindrical electrode that is considered in developing the theory.

From Maxwell's equations, since the divergence of a curl of any vector is identically zero, we get

$$\text{divcul}\mathbf{H} = \text{div}\mathbf{J} + \text{div}\frac{\partial \mathbf{D}}{\partial t} = 0 \quad \text{..... (4.12)}$$

Consequently,

$$\text{div}\mathbf{J}_f = -\text{div}(\frac{\partial \mathbf{D}}{\partial t}) \quad \text{..... (4.13)}$$

Inherent in Maxwell's equations is the principle of concentration of electric charge

$$\text{div}\mathbf{J}_f = -\frac{\partial \rho_f}{\partial t}$$

and so equation (4.13) may be expressed in the form

$$-\frac{\partial \rho_f}{\partial t} = -\text{div}(\frac{\partial \mathbf{D}}{\partial t}) \quad \text{..... (4.14)}$$

Integrating equation (4.14) in the closed surface within the charged cylindrical electrode defined by the broken line in figure 4.1 we get

$$\int_v \frac{\partial \rho_f}{\partial t} dv = \int_v \text{div}\frac{\partial \mathbf{D}}{\partial t} dv \quad \text{..... (4.15)}$$

where v is the volume of the closed surface. Consequently, the free charge density ρ_f and the free current density $\mathbf{J}_f$ in the closed surface are the conduction charge density and the conduction current density, respectively. This free current in the closed volume will flow through the air to the electrode and so

$$\int_v \frac{\partial \rho_f}{\partial t} dv = i = \frac{\partial q}{\partial t} \quad \text{..... (4.16)}$$

Thus, we have

$$\frac{\partial q}{\partial t} = \int_v (\text{div}\frac{\partial \mathbf{D}}{\partial t}) dv \quad \text{..... (4.17)}$$

It should be noted that the displacement, **D**, is a vector. The volume integral may be transformed into a surface integral where the integration surface, the broken line in figure 4.1, is defined by the following boundaries.

S1 A lateral cylindrical surface of area S_1

S2 A plane surface intersecting the liquid jet at the entrance of the electrode. The intersection surface S_2 is the cross sectional area of the liquid jet.

S3 Either, when the jet breaks up inside the electrode or exactly at its exit, a plane surface intersecting the jet disintegration point. In this case, the intersection surface S_3 is the cross sectional area within the inner surface of the electrode.

Or, alternatively, when the jet breaks up downstream of the electrode, a plane surface intersecting the liquid jet at the exit of the electrode. In this case, the intersection surface S_3 is the cross sectional area of the liquid jet.

According to the Gaussian divergence theorem

$$\int_v \mathrm{div}\left(\frac{\partial \mathbf{D}}{\partial t}\right) dv = \oint_s \frac{\partial \mathbf{D}}{\partial t} dS \quad \text{..... (4.18)}$$

Noting that

$$dS_1 = 2\pi r_j \cdot dL_j$$

$$E_a = J_f / \sigma, \quad \int J_f dS_2 = -\partial q / \partial t \quad \text{..... (4.19)}$$

we obtain the following equation

$$\frac{\partial q}{\partial t} + \tau \frac{\partial^2 q}{\partial t^2} = \varepsilon_0 E_j p_j v \quad \text{..... (4.20)}$$

where $p_j = 2\pi r_j$ is the perimeter of liquid jet, $v = dL_j / dt$ is the velocity of the liquid jet passing through the electrode and $\tau = \varepsilon_0 \varepsilon_r / \sigma$ is the relaxation time of the liquid.

Equation (4.20) is the mathematical representation of the charging rate of a liquid jet based upon Maxwell's equations. As in the case of the solution of the mathematical model based upon an equivalent electric circuit (sec. 4.3), we first need to find a general solution and then a particular one. The general solution, obtained by standard methods, is

$$q = q_h + q_k = c_3 + c_2 e^{-t/\tau} + \varepsilon_0 E_j p_j v t \quad \text{..... (4.21)}$$

where c_2 and c_3 are constants.

4.4.2 Charge on liquid jet

The charge on the liquid jet is given by a particular solution of the mathematical model which may be obtained by substituting the initial condition $q = 0$ and $\partial q / \partial t = 0$ at $t = 0$ into the general solution. Making the substitution in equation (4.21) we obtain

$$q = -\varepsilon_0 E_j p_j v\tau(1 - e^{-t/\tau} - t/\tau) \quad \text{..... (4.22)}$$

Equation (4.22) is the charge on the surface of the liquid jet inside the charged cylindrical electrode induced by the electric field at time t. The charge time of the liquid jet is given by

$$t = L_j / v \quad \text{..... (4.23)}$$

where L_j is the unbroken length of liquid jet inside the electrode and where $0 \le L_j \le L_c$.

4.4.3 Specific charge of liquid jet and charge to mass ratio

By dividing equation (4.22) by the density of the jet liquid ρ_l, we obtain an expression for β_0, the charge to mass ratio of the spray, as follows

$$\beta_0 = q / m_t = -\varepsilon_0 E_j p_j \frac{v}{Q_l \rho_l} \frac{\tau}{t}(1 - \exp(-t/\tau) - t/\tau) \quad \text{..... (4.24)}$$

Alternatively, by dividing equation (4.22) by the volume of the liquid jet given by $V_b = Q_l t = Q_l L_j / v$, we derive an expression for q_{sc}, the specific charge of the liquid jet,

$$q_{sc} = -\varepsilon_0 E_j p_j \frac{v}{Q_l} \frac{\tau}{t}(1 - \exp(-t/\tau) - t/\tau) \quad \text{..... (4.25)}$$

4.5 VELOCITY OF TIP OF LIQUID JET PASSING THROUGH ELECTRODE

It will be noted that equations (4.10) and (4.24) include the velocity v of the tip of the liquid jet. In order to obtain an expression for v it is necessary to consider the hydrodynamics of liquid jet disintegration under the influence of the atomising air.

Following the methods devised by Artana *et al*, it has been found that the velocity of the tip of the liquid jet as it passes through the charged cylindrical electrode is given by

$$v = \frac{\alpha \rho_a A_a}{\dot{m}_l}\left(\frac{\dot{m}_a}{\rho_a A_a} - \frac{\dot{m}_l}{\rho_l A_l}\right)^2 + V_l \quad \text{..... (4.26)}$$

and that the maximum value of α may be calculated from

$$\alpha_{\max} = 1 - \left(1 + \frac{\dot{m}_l}{\dot{m}_a}\right)^{-\frac{1}{2}} \quad \text{..... (4.27)}$$

Pending the development of the new theory of jet disintegration, the value of α used for computational purposes has been obtained from equation (4.27) using experimentally determined values of $\dot{m}_l$ and $\dot{m}_a$.

4.6 EQUIVALENCE OF THE THEORETICAL MODELS

Rearranging equation (4.24) in accordance with the relationship between electric field and voltage we get

$$E_j = \frac{V}{r_j \ln(r_c / r_j)} \quad \text{.....(4.28)}$$

Substitution of the following expressions into equation (4.28)

$$C = \frac{2\pi\varepsilon_0}{\ln(r_c / r_j)} L_j$$

$$L_j = vt \quad \text{.....(4.29)}$$

$$p_j = 2\pi r_j$$

leads to

$$\beta_0 = q / m_t = -\frac{C_l V}{\rho_l Q_l} \cdot \frac{\tau}{t} \cdot (1 - \exp(-t/\tau) - \frac{\tau}{t}) \quad \text{.....(4.30)}$$

Provided that, in equation (4.30), the term $t >> \tau$ or, in equation (4.10) above, the term $t >> R_l C$, then equations (4.30) and (4.10) both reduce to be the same form, namely

$$\beta_0 = q / m_t = \frac{C_l V}{\rho_l Q_l} \quad \text{.....(4.31)}$$

The only parameter that significantly influences the charge relaxation time and resistance of the jet is the conductivity (or resistivity) of the spray liquid the value of which may vary by many orders of magnitude. However, assuming that the spray liquid is water with a conductivity exceeding $\sigma = 10^{-5}\text{S/m}$, then, over the practical range of values of other water parameters and of spray nozzle electrical and geometrical parameters, the inequalities $t >> \tau$ and $t >> R_l C$ can be shown to hold.

Consequently, for water of the conductivity exceeding $\sigma = 10^{-5}\text{S/m}$, the two theoretical models have been demonstrated to be equivalent.

4.7 CHARGE ON INDIVIDUAL DROPLETS

The jet disintegration mechanism of Artana *et al* (sec. 4.5) assumes that the charge that has been induced onto the surface of the liquid jet is maintained as the coaxial ring of liquid is detached. The droplets that are then formed contain the same charge as was present on the ring. It is then assumed that the charge on the jet is uniformly distributed between the droplets such that there is the same charge per unit surface area of formed droplets. The charge q_d on

individual droplets can thus be obtained by dividing the total spray charge by the total surface area of droplets and then multiplying by the surface area of individual droplets. Consequently, we get

$$q_d = \frac{q}{S_0} \cdot \pi D^2$$
$$= \frac{6mq}{\rho_l D_{32}} \cdot \pi D^2 \quad \text{..... (4.32)}$$

4.8 LIMITATION UPON VOLTAGE APPLIED TO THE INDUCTION ELECTRODE

There is a limitation upon the voltage that may be applied to the electrode for effective induction charging. This upper bound occurs when the electrical potential at the induction electrode is sufficiently high for the electric field to exceed the electrical breakdown strength of the air and, consequently, for corona discharge to take place. Droplets within the induction electrode then receive some charge by ion bombardment.

Unfortunately, the polarity of the charge is opposite to that generated by induction and the effect is to reduce the charge on the droplets.

The corona-starting voltage is given by

$$V_0 = r_j E_c \ln(r_c / r_j) \quad \text{..... (4.33)}$$

and the corona starting field strength E_c can be calculated, for negative corona, by

$$E_c = f_r(31.02\delta_a + 9.54\times10^{-1}\sqrt{\frac{\delta_a}{r_j}})\times10^5 \quad \text{..... (4.34)}$$

and for positive corona, by

$$E_c = f_r(33.7\delta_a + 8.13\times10^{-1}\sqrt{\frac{\delta_a}{r_j}})\times10^5 \quad \text{..... (4.36)}$$

where f_r is a roughness factor the value of which, for practical purposes, lies in the range 0.5 to 0.9. Thus, equations (4.34), (4.35) and (4.36) establish an upper bound for corona-free operation for any coaxial-electrode, induction-charged air-atomising nozzle.

4.9 THEORETICAL CALCULATIONS OF SPRAY AND DROPLET CHARGE

It will be evident from the theory set out above that there are a large number of parameters which influence spray and droplet charge. During the series of experiments described below in chapter five, three of the most significant parameters were varied, namely

a. air flowrate Q_a,

b. spraying liquid (water) flowrate Q_l and

c. applied voltage V.

The effect upon spray and droplet charge of the variation in the values of these three parameters was also studied theoretically.

Values of other parameters were fixed, for both theoretical and experimental purposes, as follows.

a. Geometrical parameters
   - Diameter of nozzle orifice and liquid jet d = 1.02mm
   - Radius of induction charging electrode r_C =1.78 mm
   - Length of induction charging electrode L_C =1.27 mm

b. Environmental parameters
   - Standard temperature and pressure, i.e. t = 15°C & P = 101.325 kPa

c. Air parameters
   - Density ρ_a = 1.225 kg/m^3

d. Liquid (water) parameters
   - Conductivity $\sigma = 10^{-2}$ S/m
   - Density $\rho_l = 1000 kg/\mathrm{m}^3$
   - Dielectric constant $\varepsilon_r = 80.4$
   - Resistivity ρ =100 Ωm
   - Surface tension $\sigma_l = 0.0747 \mathrm{N/m}$
   - Viscosity $\mu_l = 0.001 \mathrm{Ns/m}^2$

The air-jet interaction coefficient α (sec. 4.5) was taken as $0.7\alpha_m$ for the calculation of induction charging for both theoretical and experimental purposes.

In addition, the following simplifying, but not invalidating, assumptions were introduced in the calculation of spray charge-to-mass ratio.

a. The geometry is such that the break up of the liquid jet always takes place at the end of, or a little downstream of, the cylindrical electrode.

b. The jet does not deteriorate inside the cylindrical electrode.

c. The charge on the jet does not influence the hydrodynamics of jet break up.

Both theoretical models being mathematically equivalent, the following computations were all based upon equation (4.24) which was derived by the Maxwell's equations method.

4.9.1 Charge-to-mass ratio of liquid jet

4.9.1.1 Effect of air velocity and liquid flowrate

Figure 4.3 presents the relationship between spray charge-to-mass ratio and liquid flowrate at several different air velocities for an applied voltage V of 1000 volts.

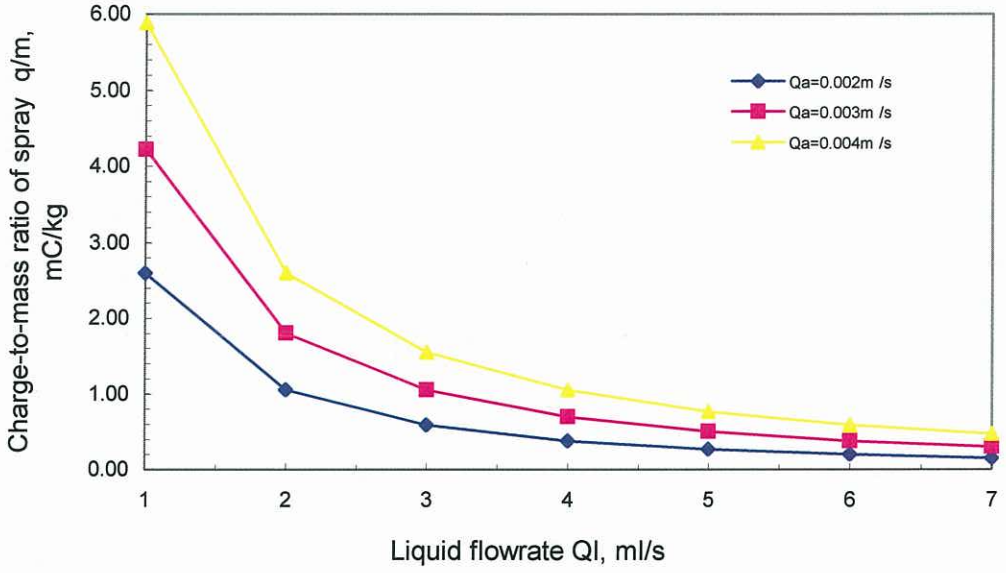

Fig. 4.3 Effect of air velocity and liquid flowrate on spray charge-to-mass ratio

It will be seen that the spray charge-to-mass ratio decreases with increasing liquid flowrate, the rate of decrease being particularly evident at lower liquid flowrates. As the charge transfer time constant for water is much less than the residency time, decreasing the residency time by increasing the liquid flowrate will not prevent the liquid jet from being satisfactorily charged. However, the increased quantity of liquid passing through the electrode will acquire the same charge in unit time resulting in a lower charge-to-mass ratio.

It is also evident that the spray charge-to-mass ratio increases with increasing air velocity. The reason for this is that an increase in air velocity causes the tip of the liquid jet to pass through the cylindrical electrode with a higher velocity. This, in turn, results in a higher spray charge-to-mass ratio.

It should be noted, however, that the theoretical calculations are based upon the assumption that jet disintegration takes place at or beyond the exit from the cylindrical electrode. If the air velocity were too high or the liquid flowrate too low, the jet would break up at or before the entrance to the electrode. In this case, no induction would take place and the spray current, and charge-to-mass ratio, would be zero. Consequently, the models for induction-charged air-atomising nozzles do not hold for very high air velocities or very low liquid flowrates.

4.9.1.2 Effect of applied voltage

Figure 4.4 shows the effect of variations in the applied voltage on the charge-to-mass ratio of the liquid spray for several combinations of air velocity and liquid flowrate.

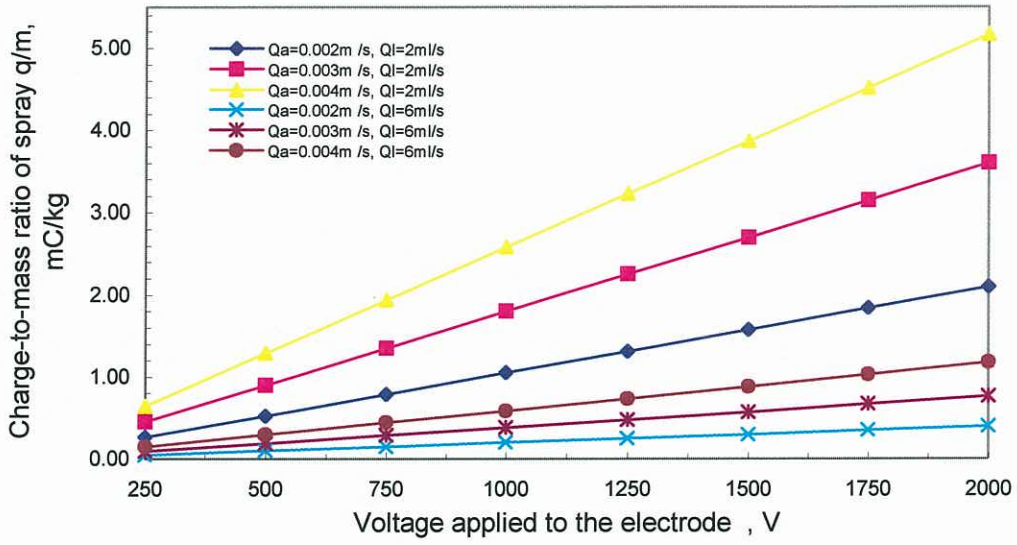

Fig. 4.4 Effect of applied voltage on spray charge-to-mass ratio

As the applied voltage on the induction electrode increases, the field strength increases, more charge, of a polarity opposite to that of the electrode, is induced onto the spray and its charge-to-mass ratio increases. The rate of increase in charge-to-mass ratio with increasing applied voltage is more marked at higher air velocity / liquid flowrate quotients.

All the lines in figure 4.4 suggest that the spray charge-to-mass ratio increases linearly with the applied voltage. However, in practice, several phenomena could cause possible deviations from the idealised induction charging models.

Firstly, some of the droplets that are formed could wet the induction electrode. Any such liquid deposited on this high-voltage electrode could be drawn into a sharp discharge peak by the electric field and this would result in an ion current flowing back onto the charged liquid jet. Because of its opposite polarity, this would tend to neutralise the charging by the electrostatic induction process.

Secondly, if the applied voltage on the induction electrode were to be raised to a value above that which would initiate gaseous breakdown and subsequent corona discharge in the air just off the surface of the jet, the electric field strength would be reduced and, consequently, the charge-to-mass ratio of the liquid spray would diminish.

A third phenomenon which, if present, could cause an increase in spray-cloud current above that predicted by the model is the electrohydrodynamic (EHD) spray effect. This could lead to the emission of highly charged droplets, of the same polarity as the induced charge, from the liquid jet due to surface disruption by stresses imposed by interaction of the surface charge and the applied field.

The above considerations indicate that there is probably an optimum voltage to which the induction electrode should be raised in order to produce the greatest spray current, higher voltages resulting in a decrease in spray current or charge-to-mass ratio. This optimum voltage may be expected to vary both with geometry and with air & liquid flowrates.

4.9.2 Charge acquired by droplets

4.9.2.1 Effect of liquid flowrate

Figure 4.5 shows the effect of variations in the liquid flowrate on droplet diameter and charge for a fixed air flowrate $Q_a = 0.003$ m^3 /s and fixed applied voltage $V = 1000$ volts.

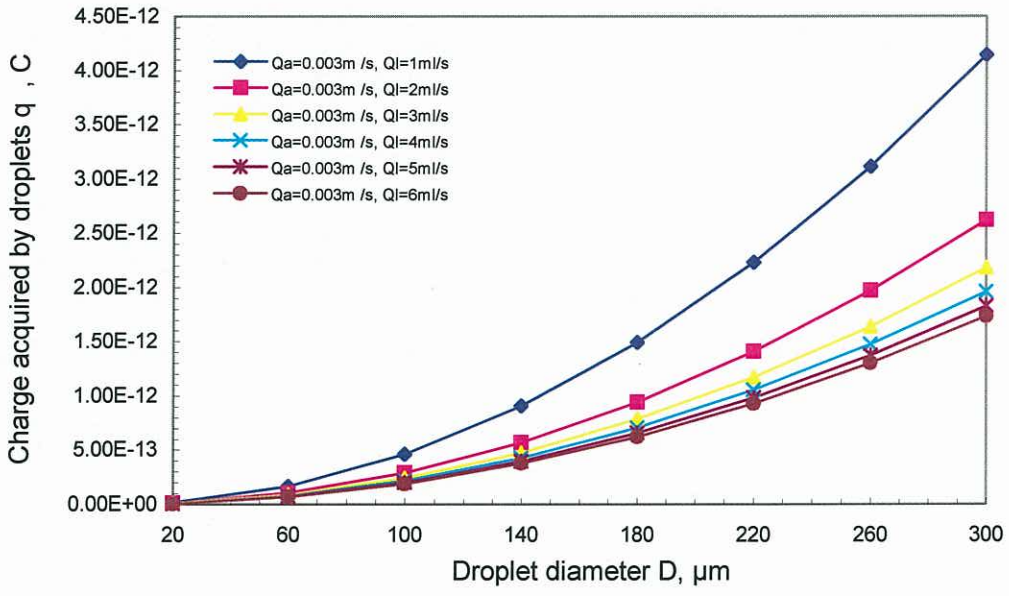

Fig. 4.5 Effect of liquid flowrate on droplet diameter and charge

The figure indicates that, for a given applied voltage and air flowrate, the predicted charge on droplets of the same size decreases with increasing liquid flowrate. While, for small droplet

sizes, the rate of increase is low, it becomes more significant as droplet size increases. The reason is that if the liquid flowrate is increased while keeping the air flowrate constant, the charge level of the spray will decrease. However, more large droplets will be produced and the Sauter mean diameter will become larger. If it is assumed that the charge on the surface of the liquid jet is uniformly distributed on the formed droplets such that there is the same charge per unit surface area of droplets, small droplets will be seen to have less charge on the surface. This leads to the charge on droplets of the same size decreasing with increasing liquid flowrate.

4.9.2.2 Effect of applied voltage

The variation of the charge acquired by the droplets is shown in figure 4.6 for different applied voltages and droplet diameters.

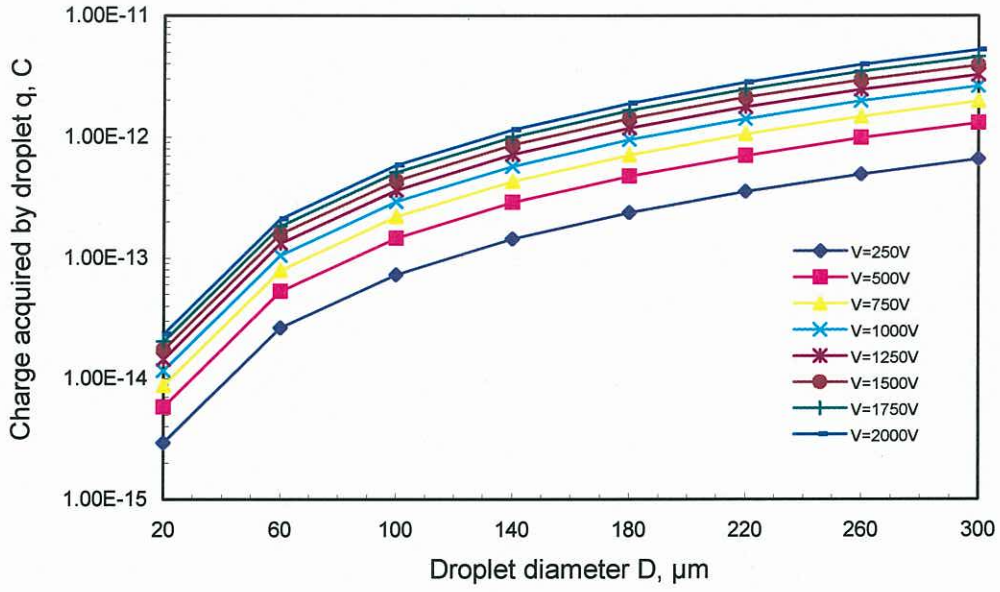

Fig. 4.6 Effect of applied voltage and droplet diameter on droplet charge

It will be seen that the charge on droplets of the same size increases with increasing applied voltage. This results from the fact that increasing the applied voltage increases the amount of charge on the surface of the liquid jet. As indicated above in section 4.9.1.2, which discusses the effect of the applied voltage on the charge-to-mass ratio of the spray, several phenomena which might well occur in practice could affect the charge level of the spray and, hence, the charge on individual droplets. Consequently, there may well be an optimum voltage at which droplets of a particular diameter would acquire maximum charge.

5 RESULTS OF LABORATORY INVESTIGATIONS

5.1 INTRODUCTION

The very extensive programme of laboratory testing undertaken as part of the Dust Suppression Project involved investigations into two separate issues.

a. The ability of the induction-charged air-atomising nozzle to impart an electrostatic charge onto water droplets.

b. The ability of such electrostatically charged water droplets to capture airborne coal dust.

5.2 RESULTS OF INVESTIGATIONS REGARDING ELECTROSTATIC CHARGING

Because of the complexity of the induction charging / air atomisation process, it was considered quite impracticable to investigate, in the laboratory, the effects of the large number of potentially relevant parameters.

Consequently, the induction-charged air-atomising nozzle and Electrostatically Charged Water Spray Collection (ECWSC) Rig, described in sections 3.2 and 3.3 respectively, were employed in a preliminary series of experiments designed to demonstrate the ability of the induction-charged air-atomising nozzle to electrostatically charge water droplets and to validate the theoretical models for the induction charging and air atomisation of a liquid jet which were outlined in chapter four. The intention was that the theoretical models, once validated, would be used as a guide in the selection of design parameters in order to optimise induction-charged air-atomising nozzle performance, further laboratory work being primarily directed at

a. investigating any parameters which were considered not to have been adequately addressed by the theory and

b. 'fine tuning' the design.

During the investigations, values of the following parameters were varied.

a. Atomising air pressure in the range 20 to 40 psi (138 to 276 kPa)

b. Liquid (water) flowrate in the range 2 to 8 mL/s (120 to 480 mL/min)

c. Applied voltage in the range 0 to 2000 volts

Values of relevant fixed parameters were generally as given in section 4.9 above.

5.2.1 Comparison of experimental results with theory

5.2.1.1 Effect of air pressure and liquid flowrate

Figure 5.1 provides a comparison of theoretically and experimentally determined values for the variation in spray charge-to-mass ratio with different air pressures and liquid flowrates at an applied voltage V that was fixed at 500 volts.

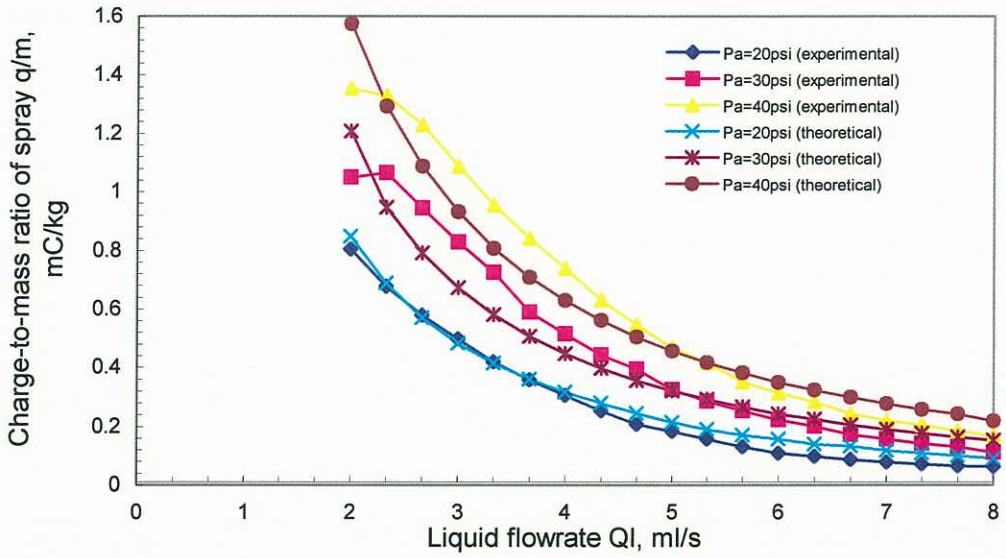

Fig. 5.1 Comparison of theory and experiment for spray charge-to-mass ratio at different air pressures and liquid flowrates

The experimental results show that, as predicted by theory (sec. 4.9.1.1), the spray charge-to-mass ratio increases with increasing air pressure (and, consequently, air flowrate) but decreases with increasing liquid flowrate. It is also evident that the theoretically and experimentally determined values are in reasonable agreement other than at low liquid flowrates.

The deviation between experimental and theoretical results, which is evident at liquid flowrates less than about 2.5 mL/s, may be due to premature jet break up inside the cylindrical charging electrode as a consequence of higher air pressures or lower liquid flowrates or a combination thereof (but see, also, section 5.2.1.2 below). However, the phenomenon is not relevant to the induction charging of sprays for dust suppression in that high liquid flowrates are envisaged in this application.

5.2.1.2 Effect of applied voltage

Experimental results

Figure 5.2 shows the experimentally determined effect of applied voltage on spray charge-to-mass ratio for varying liquid flowrates but at a fixed atomising air pressure of 40 psi (276 kPa).

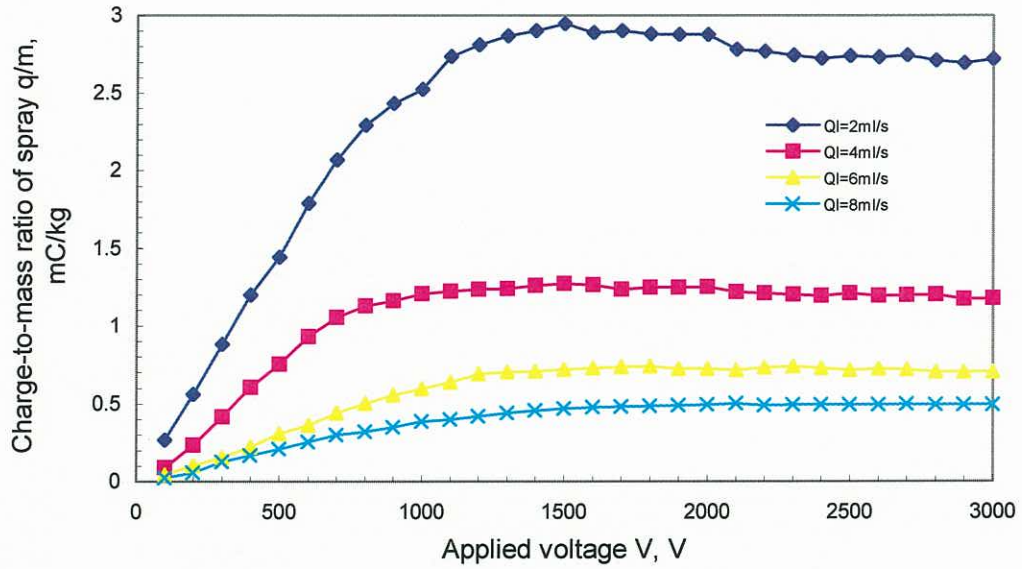

Fig. 5.2 Effect of applied voltage on spray charge-to-mass ratio for several liquid flowrates

It will be noted that for lower liquid flowrates the spray charge-to-mass ratio increases with increasing applied voltage up to a maximum and then decreases with further increases in the applied voltage, whereas for higher liquid flowrates the charge-to-mass ratio reaches an apparent 'plateau' after the initial increase.

Figure 5.3 below shows the effect of liquid flowrate on spray charge-to-mass ratio for applied voltages ranging from 500 to 2000 volts at a fixed air pressure of 40 psi (276 kPa). It will be seen that, for all values of applied voltage, the charge-to-mass ratio of the spray generally decreases with increasing liquid flowrate. As in figure 5.1, however, there is a tendency for this trend to reverse at liquid flowrates less than about 2.5 mL/s but this is only evident at 500 and 1000 volts and not at higher applied voltages. Consequently, although it was suggested in section 5.2.1.1 above that the phenomenon may be due to premature jet break up inside the electrode, it is evident that it must also have an 'electrical' component.

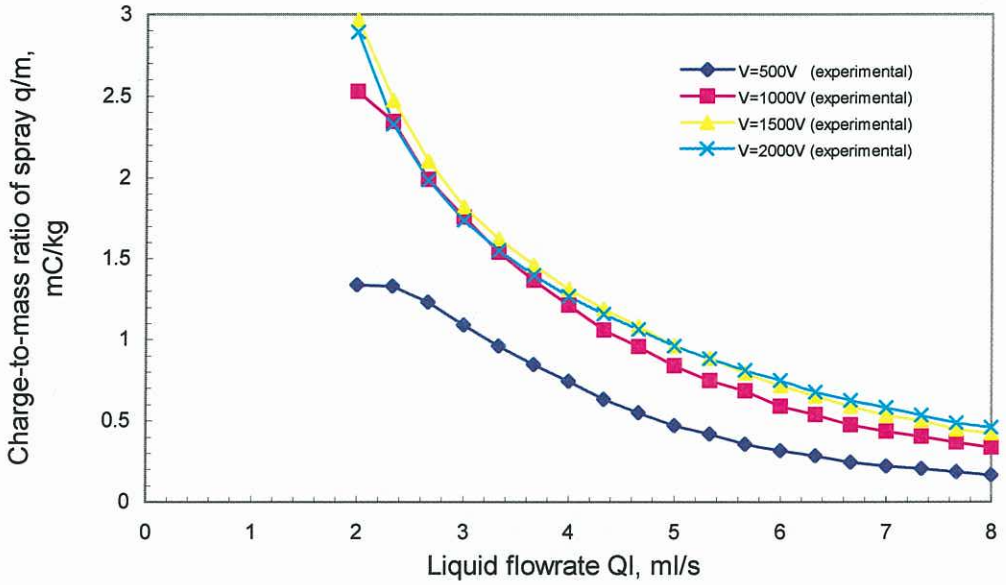

Fig. 5.3 Effect of liquid flowrate on spray charge-to-mass ratio for several applied voltages

Comparison of experimental results with theoretical predictions

Figure 5.4 shows a comparison of the theoretically and experimentally determined relationships between spray charge-to-mass ratio and liquid flowrate for a range of applied voltages at a fixed air pressure of 40 psi (276 kPa).

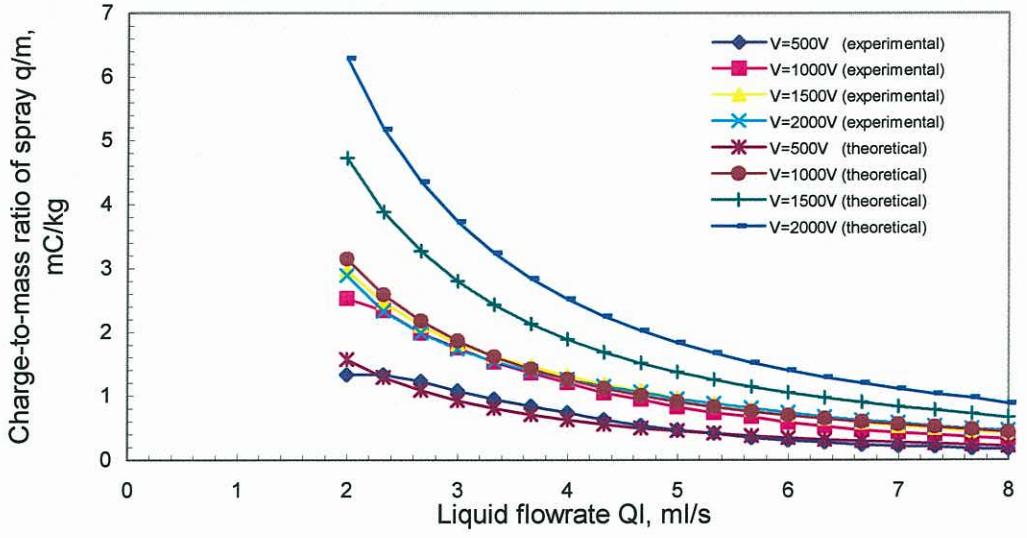

Fig. 5.4 Comparison of theory and experiment for spray charge-to-mass ratio at different liquid flowrates and applied voltages

It will be seen that although the experimental results are in good agreement with theory for applied voltages up to 1000 volts, the experimental results never reach the theoretically calculated values at the higher applied voltages of 1500 and 2000 volts. The reason for this is considered to lie in the phenomenon of corona discharge at the higher applied voltages.

Calculations based upon the equations set out in section 4.8 above indicated that the corona-starting voltage V_o for the experimental setup, assuming a 'smooth' electrode, was approximately 2000 volts. However, when the roughness factor was taken into account this value was reduced to 1200 to 1800 volts. It is postulated that at high liquid flowrates the surface shape of the liquid jet is better than at low liquid flowrates, the roughness factor is larger and, consequently, the corona starting voltage is higher. This is supported by figure 5.2 where the applied voltage corresponding to the maximum spray charge-to-mass ratio increases with increasing liquid flowrate.

The practical effect of the above is that, for any particular geometrical configuration of induction-charged air-atomising nozzle, there exists, at any given air and liquid flowrate, an optimum applied voltage which will generate the maximum spray charge-to-mass ratio. Any increase above the optimum voltage will induce no further increase in charge-to-mass ratio and may, indeed, result in a decrease.

5.2.2 Conclusions regarding the electrostatic charging of water droplets

The preliminary programme laboratory of testing demonstrated that the induction-charged air-atomising nozzle is able to impart a significant electrostatic charge onto water droplets. Furthermore, it was shown that the theoretical models of the induction-charged air-atomising nozzle are able to adequately predict its characteristics.

The spray charge-to-mass ratio was shown to increase with

a. applied voltage (to a maximum) and

b. atomising air pressure.

The spray charge-to-mass ratio was shown to decrease with water flowrate.

In addition, it was demonstrated that the induction-charged air-atomising nozzle can be operated safely in an environment of wet coal dust and that 'voltage breaking', in order to isolate the water supply from the elevated electrical potential used to apply the electrostatic charge, is unnecessary.

5.3 RESULTS OF INVESTIGATIONS REGARDING DUST CAPTURE

An extensive series of investigations was undertaken in which the Electrostatically Charged Water Spray Dust Suppression (ECWSDS) Rig (sec. 3.4) was utilised to examine the efficacy of the induction-charged air-atomising nozzle (sec. 3.2) in suppressing both inspirable and respirable dust and to investigate the effects of the principal design and operational variables on dust suppression efficiency.

During the investigations, values of the following parameters were varied.

a. Applied voltage in the range 0 to 3000 volts
b. Coal dust concentration in the range 30 to 500 mg per cubic metre of air
c. Air velocity through the 'test section' of the ECWSDS Rig in the range 0.5 to 1.25 metres per second
d. Water flowrate in the range 2 to 8 mL/s (120 to 480 mL/min)
e. Atomising air pressure in the range 20 to 70 psi (138 to 483 kPa)

Values of other relevant parameters were generally as given in section 4.9 above.

5.3.1 Experimental results regarding dust suppression efficiency

5.3.1.1 Effect of applied voltage

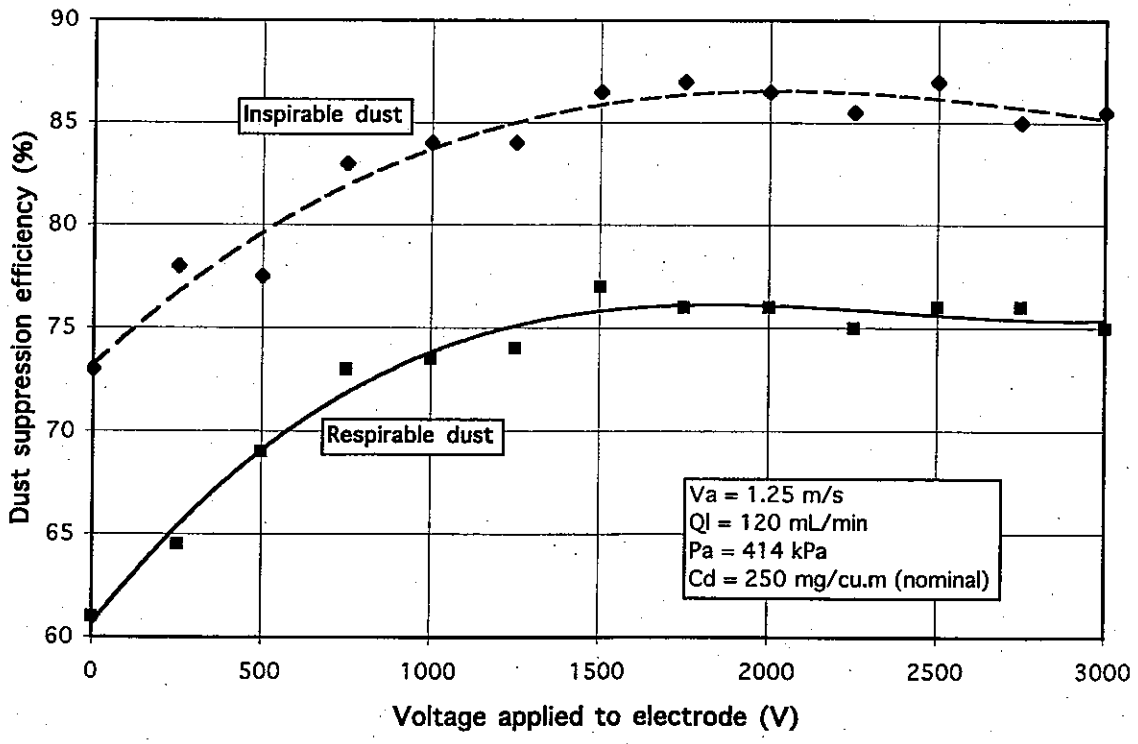

Fig. 5.5 Effect of applied voltage on coal dust suppression efficiency

Figure 5.5 above shows the experimentally determined relationship between applied voltage and dust suppression efficiency for both inspirable and respirable dust. Testing was undertaken at a fixed water flowrate of 120 mL/min, an atomising air pressure of 60 psi (414 kPa) and an air velocity through the 'test section' of 1.25 m/s.

The concentration of coal dust in the body of the ECWSDS Rig immediately prior to the air entering the 'test section' was nominally 250 mg/m^3. However, for a given air velocity, the concentration was controlled by adjusting the feed rate of the dust (sec. 3.4.1.2) and so the exact value could only be determined, by gravimetric means, after completion of the test run. Consequently, it was necessary to accept some variation in the value of coal dust concentration from the nominal value and, for practical purposes, a range of ±20 mg/m^3 was accepted. This meant that a test run was regarded as valid, and the data accepted, provided the coal dust concentration was between 230 and 270 mg/m^3. The implication of a variation of ±20 mg/m^3 in the concentration of coal dust upon suppression efficiency is discussed in section 5.3.1.2 below.

It will be observed from figure 5.5 that inspirable dust was suppressed more effectively than was respirable dust, the difference in suppression efficiency ranging from 10 to 12 per cent. For both dust types, however, the effect of electrostatically charging the water droplets was to substantially improve the dust suppression efficiency of the spray. The efficiency reached a maximum at around 1750 to 2000 V and then decreased slightly as the voltage applied to the induction electrode was further increased. The effect is tabulated in figure 5.1.

Table 5.1 Effect of applied voltage on coal dust suppression

Coal dust type	*Suppression efficiency of uncharged spray*	*Suppression efficiency of optimally charged spray*	*Reduction in unsuppressed dust*
	%	%	%
Inspirable dust	73.0	86.5	50
Respirable dust	61.0	76.5	40

It will be seen from table 5.1 that the effect of electrostatically charging the spray was to reduce the concentration of the remaining, unsuppressed inspirable dust by 50 per cent compared with the uncharged case while in the case of respirable dust the reduction was 40 per cent.

It will be noted from section 3.5.1.6 that the best accuracy was achievable when the maximum coal dust load, of the order of 30 mg, was collected on the filter membrane. The coal dust load on the 'downstream' filter was, of course, much less than on the 'upstream' filter and the

minimum dust load in the data set from which figure 5.5 was derived was of the order to 4 mg. The 'acceptance criterion' (sec. 3.5.1.7) for dust laden filters was ±20 μg and, consequently, an accuracy of ±0.5% in the determination of the weight of coal dust was the best that was theoretically achievable.

It is of interest to compare figure 5.5 with figure 5.2 which shows the effect of applied voltage on spray charge-to-mass ratio. The shape of the curves is generally similar suggesting that the ability of the electrostatically charged water droplets to suppress coal dust is closely related to the spray charge-to-mass ratio. This is also borne out by the conclusion of Cross and Smith (1994), based upon numerical modelling of water sprays, that dust suppression effectiveness increases with electrostatic charge.

5.3.1.2 Effect of coal dust concentration

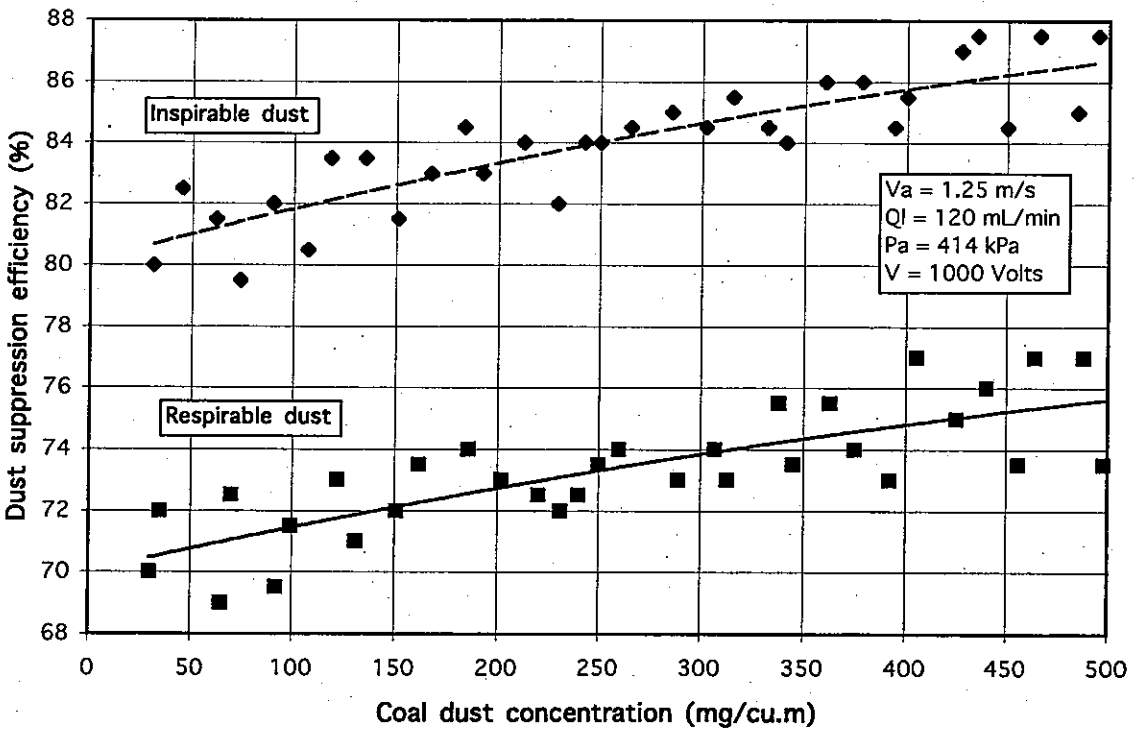

Fig. 5.6 Effect of coal dust concentration on suppression efficiency

Figure 5.6 shows the effect of coal dust concentration on suppression efficiency for both inspirable and respirable dust. The values of coal dust concentration on the abscissa are the actual values determined by gravimetric means after completion of the test run. Consequently, the values are not evenly distributed. Testing was undertaken at a fixed water flowrate of 120 mL/min, an atomising air pressure of 60 psi (414 kPa), an air velocity through the 'test section' of 1.25 m/s and an applied voltage of 1000 volts.

It will be observed that the relationship between coal dust concentration and dust suppression efficiency was almost linear for both types of coal dust, suppression efficiency decreasing with increasing dust concentration. Inspirable dust was suppressed more effectively than was respirable dust, the difference in suppression efficiency being of the order of ten per cent.

The minimum coal dust load on the 'downstream' filter in the data set from which figure 5.6 was derived was of the order to 1000 μg. The 'acceptance criterion' (sec. 3.5.1.7) for dust laden filters was ±20 μg and, consequently, an accuracy of ±2% in the determination of the weight of coal dust was the best that was theoretically achievable.

It is mentioned in section 5.3.1.1 above that a variation of ±20 mg/m^3 in the value of coal dust concentration was accepted for the purpose of determining the effect of applied voltage upon dust suppression efficiency. It may be calculated from figure 5.6 that the corresponding variation in the value of dust suppression efficiency is ±0.25%.

5.3.1.3 Effect of air velocity

The effect of the velocity of air passing through the 'test section' of the ECWSDS Rig on suppression efficiency is shown in figure 5.7 for both inspirable and respirable dust. Testing was undertaken at a fixed water flowrate of 120 mL/min, an atomising air pressure of 60 psi (414 kPa), a nominal dust concentration (see sec. 5.3.1.2) of 250 mg/m^3 and an applied voltage of 1000 volts.

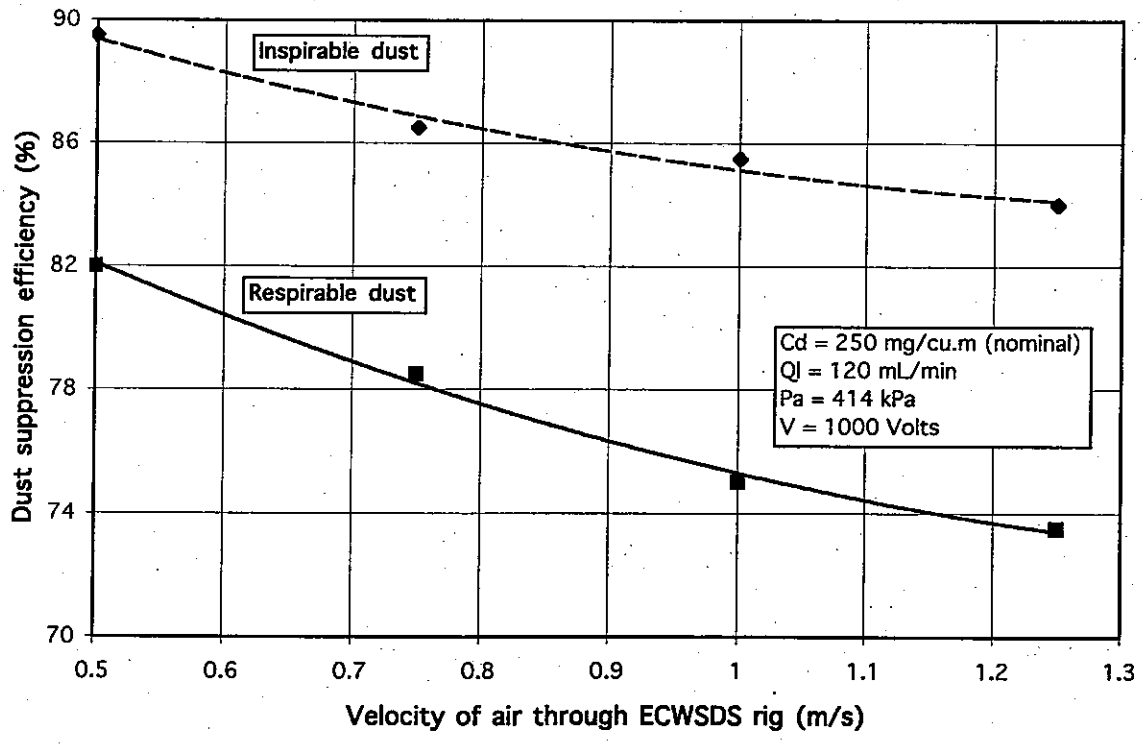

Fig. 5.7 Effect of air velocity on coal dust suppression efficiency

The relationship between air velocity through the ECWSDS Rig and dust suppression efficiency will be observed to be effectively linear for both types of coal dust, suppression efficiency increasing with decreasing air velocity. The reason is believed to be the increased time for the air to traverse the spray zone and, hence, the increased interaction time between the dust particles and the electrostatically charged water droplets (Cross and Smith 1994).

Inspirable dust was suppressed more efficiently than was respirable dust, the difference in suppression efficiency being of the order of ten per cent.

5.3.1.4 Effect of atomising air pressure

Figure 5.8 shows the effect of the pressure of the air applied to the induction-charged air-atomising nozzle on suppression efficiency for both inspirable and respirable dust. Testing was undertaken at a fixed water flowrate of 120 mL/min, an air velocity through the 'test section' of 1.25 m/s, a nominal dust concentration (see sec. 5.3.1.2) of 250 mg/m^3 and an applied voltage of 1000 volts.

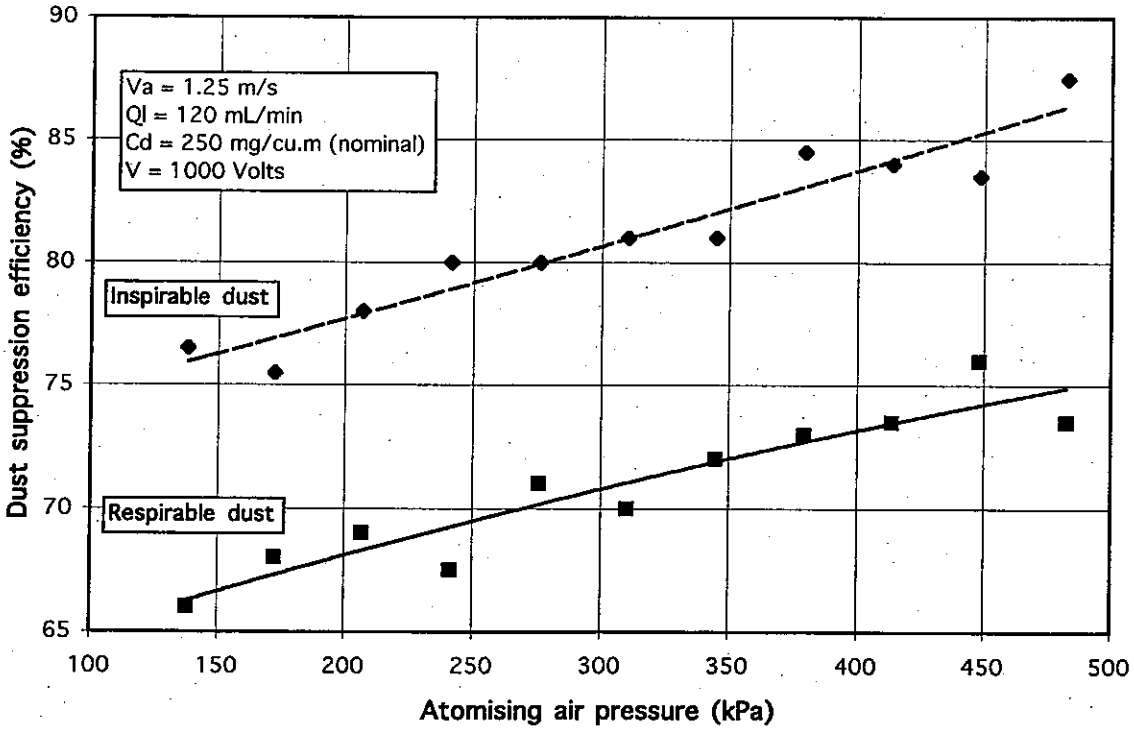

Fig. 5.8 Effect of atomising air pressure on coal dust suppression efficiency

It will be observed that the relationship between atomising air pressure and dust suppression efficiency is effectively linear for both types of coal dust, suppression efficiency increasing

with increasing air pressure. Inspirable dust was suppressed more efficiently than was respirable dust, the difference in suppression efficiency being of the order of 10 per cent.

In this context, it is of interest to examine figure 5.1 which is based upon both theoretical and experimental results and indicates that, for a given liquid (water) flowrate, the effect of increasing the atomising air pressure is to increase the spray charge-to-mass ratio. This appears to reinforce the conclusion (sec. 5.3.1.1) that dust suppression effectiveness increases with electrostatic charge.

5.3.1.5 Effect of water flowrate

The effect upon suppression efficiency of the rate of flow of water through the induction-charged air-atomising nozzle is illustrated by figure 5.9 for both inspirable and respirable dust. Testing was undertaken at a fixed air velocity through the 'test section' of 1.25 m/s, a nominal dust concentration (see sec. 5.3.1.2) of 250 mg/m^3, an atomising air pressure of 60 psi (414 kPa) and an applied voltage of 1000 volts.

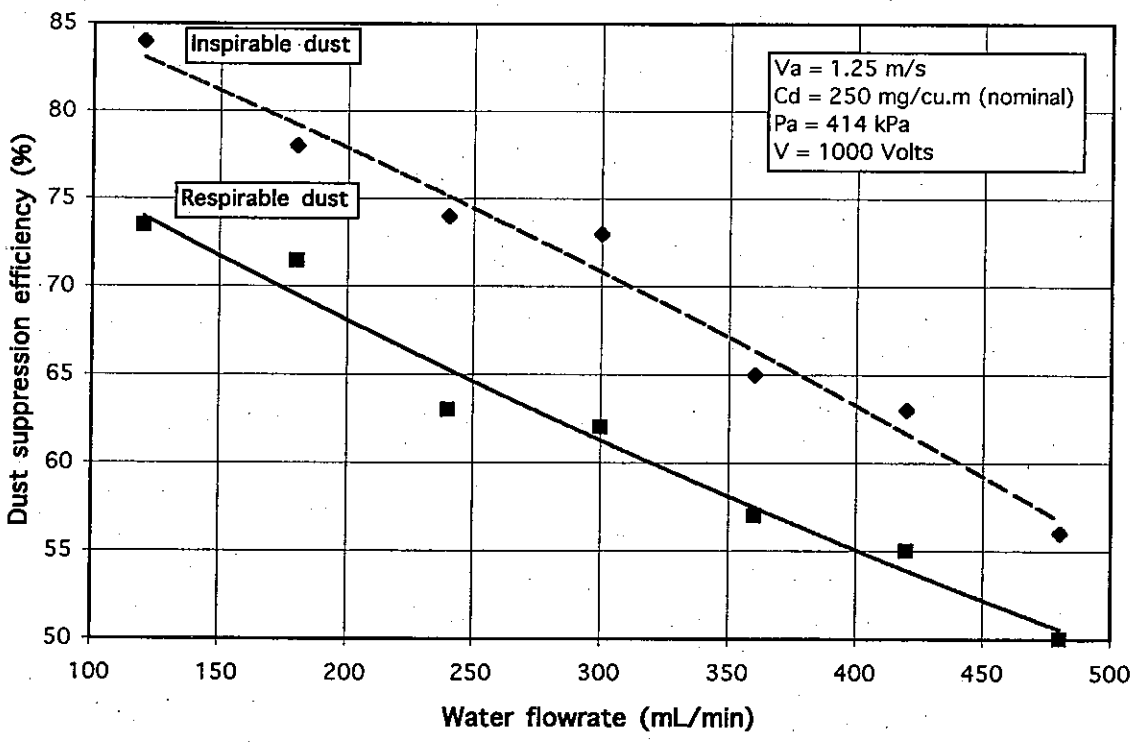

Fig. 5.9 Effect of water flowrate on coal dust suppression efficiency

The relationship between water flowrate and dust suppression efficiency will be observed to be effectively linear for both types of coal dust, suppression efficiency decreasing with increasing water flowrate.

At first sight, this result would appear to be run counter to the conclusion of Cross and Smith (1994), based upon numerical modelling of water sprays, that, for a given droplet size and charge-to-mass ratio, the dust suppression effectiveness of electrostatically charged water sprays increases with increasing water flowrate. The explanation for the apparent anomaly may ascertained by comparing figure 5.9 with figure 5.1 which indicates that the effect of increasing the liquid flowrate is to reduce the spray charge-to-mass ratio. Xiao (2000) also showed that the effect of increasing the liquid flowrate is to reduce the total spray current. It may be concluded from figure 5.9 that the increase in water flowrate does not compensate for the reduction in spray current.

As in the case of the other variables whose effect on dust suppression efficiency was considered in sections 5.3.1.1 to 5. 3.1.4, inspirable dust was suppressed more efficiently than was respirable dust, the difference in suppression efficiency being of the order of 10 per cent.

5.3.2 Conclusions regarding coal dust capture

The extensive programme of laboratory testing has demonstrated the ability of electrostatically charged water droplets to capture airborne coal dust. Coal dust concentrations passing through the Electrostatically Charged Water Spray Dust Suppression (ECWSDS) Rig were significantly reduced by the electrostatically charged spray generated by the induction-charged air-atomising nozzle.

The effectiveness of coal dust capture was shown to increase with

a. applied voltage (to a maximum),
b. coal dust concentration and
c. atomising air pressure.

The effectiveness of coal dust capture was shown to decrease with

a. air velocity through the ECWSDS Rig and
b. water flowrate.

In all instances, inspirable dust was captured more efficiently than was respirable dust.

6 CONCLUSIONS AND FURTHER WORK

6.1 CONCLUSIONS

The objectives of Stage 2 of the Dust Suppression Project have been achieved. The principal findings are outlined below.

6.1.1 Design constraints and criteria

As the result of an extensive programme of consultation with industry, equipment manufacturers and regulatory authorities, design issues and constraints were identified for a practical and safe electrostatically charged water spraying system, suitable for industrial applications such as mounting on a longwall shearer in an underground coal mine. A set of design criteria for efficient dust suppression was drawn up and a safety assessment undertaken. Induction charging was identified as the preferred charging technique and air atomisation as the preferred atomisation technique.

6.1.2 Spraying systems

Sources of electrostatically charged spraying systems that had been developed for electrostatic operation were identified and a list of commercially available equipment was drawn up. It was considered, however, that none of these adequately fulfilled the design constraints and criteria. Consequently, it was decided that electrostatic charging functionality would be added to a commercial, non-electrostatic spraying system. A list of sources of non-electrostatic systems that had the potential to be adapted was compiled, the devices assessed and a preferred device selected.

6.1.3 Development of induction charging and atomisation theories

Because of the complexity of the induction charging / air atomisation process and the large number of parameters which could potentially effect its efficiency, a rigorous theory with which to guide the laboratory investigations and design process was essential. However, following an extensive review of the literature, existing theories for the induction charging and air atomisation of a liquid jet were found to be inadequate. Consequently, new theories were developed which describe the charging of a liquid jet by induction and the hydrodynamics of liquid jet disintegration under the influence of atomising air. This task was additional to the original scope of Stage 2 of the Dust Suppression Project.

6.1.4 Laboratory testing

An item of laboratory test equipment, the Electrostatically Charged Water Spray Collection (ECWSC) Rig was designed and constructed in order to facilitate the testing of

electrostatically charged water spraying devices and the measurement of spray current and spray cloud parameters. In addition, a second major item of laboratory equipment, the Electrostatically Charged Water Spray Dust Suppression (ECWSDS) Rig, was developed for the purpose of investigating the ability of electrostatically charged water droplets to capture airborne coal dust.

The induction-charged air-atomising nozzle that had been selected as the preferred device was employed in a preliminary series of experiments that was undertaken using the ECWSC Rig. The primary objective, the validation of the newly developed theory, was achieved. It was also demonstrated that the induction-charged air-atomising nozzle is able to impart a significant electrostatic charge onto water droplets.

The ECWSDS Rig was employed in an extensive series of experiments that investigated the effects of the principal design and operational variables on dust suppression efficiency. It was demonstrated that unsuppressed coal dust, both inspirable and respirable, can be almost halved by the addition of electrostatic charge to the water spray. Furthermore, it was shown that an electrostatically charged water spray dust suppression system can be operated safely in an environment of wet coal dust.

6.2 FURTHER WORK

The further work that is to be undertaken as part of Stage 3 of the Dust Suppression Project is summarised below.

6.2.1 Dusts other than coal

The effectiveness of electrostatically charged water spray in capturing dusts other than coal will be examined.

6.2.2 Design of prototype industrial system

A final design is to be prepared for an electrostatically charged water spraying system suitable and safe for industrial use, particularly at the coal face in underground mines.

6.2.3 Feasibility study and risk assessment

A feasibility study and risk assessment will be undertaken into the application of the prototype electrostatically charged water spraying system at the coal face.

6.2.4 Construction and demonstration of the prototype industrial system

The prototype system will be built and demonstrated in field trials, preferably on a longwall shearer in an underground coal mine.

7 TECHNOLOGY TRANSFER

Personnel from mining and quarrying companies, equipment manufacturers and regulatory authorities were interviewed in a round of consultations with industry with the aim of identifying system design issues and constraints.

Interim project reports on the electrostatic enhancement of water sprays for coal dust suppression were issued in April 1994 (Cross & Smith 1994) and October 1998 (Cross, Fowler & Xiao 1998). They are available as ACARP (Australian Coal Association Research Program) publications from Australian Research Administration Pty Ltd, Brisbane.

Presentation on the electrostatic enhancement of water sprays for coal dust suppression were made to the Standing Committee on Dust Research and Control in February 1996 and April 2001.

Informal discussions were held at those underground coal mines where 'dust problems' had been identified.

It is also anticipated that this report will be widely disseminated.

This page intentionally blank

8 ACKNOWLEDGEMENTS

The Authors wish to extend their sincere thanks to the following persons and organizations for directly or indirectly contributing to the success of the Dust Suppression Project:

The project leaders, Prof. JA Cross, former Head of the School of Safety Science, The University of New South Wales, and Prof. FF Roxborough, former Head of the School of Mining Engineering, The University of New South Wales, for ably directing the project as well as generously providing help and assistance;

Prof. JM Galvin, former Head of the School of Mining Engineering, The University of New South Wales, for making available the facilities of the School;

Assoc. Prof. C Winder, Head of the School of Safety Science, The University of New South Wales, for making available the facilities of the School;

Assoc. Prof. N Aziz, Faculty of Engineering, University of Wollongong, for kindly making available the dust injector;

Mr P Smith, former Research Assistant, The UNSW School of Safety Science, for undertaking the numerical modelling of coal dust capture by both charged and uncharged water sprays;

Mr Fuchun Xiao, former PhD student, The UNSW School of Safety Science, for undertaking the analytical modelling of induction charging described in section 4 and the laboratory investigations into induction charging described in section 5.2;

Mr W Eggermont, former Foreman, The UNSW Mining Engineering workshop, and his staff for the construction of equipment;

Other members of the staff of The University of New South Wales who assisted in various ways;

Mr G Hansen, Minerals Research Laboratories, CSIRO Exploration and Mining, and his staff for providing the finely milled coal; and

The National Energy Research, Development and Demonstration Council, the Australian Research Council, Australian Coal Research Limited (Australian Coal Association Research Program) and the Joint Coal Board Health & Safety Trust for providing financial support for the Dust Suppression Project.

The Authors also wish to acknowledge Spraying Systems Co. for permission to reproduce figure 3.1.

This page intentionally blank

9 REFERENCES

Artana, G, Bassani, LC & Scaricabarozzi, R 1992, 'Specific charge of induction electrified sprays', *Journal of Electrostatics,* vol. 29, pp. 127-145.

Atten, A & Oliveri, S 1992, 'Charging of drops formed by circular jet break up', *Journal of Electrostatics,* vol. 29, pp. 73-91.

Cross, JA 1987, Electrostatics principles problems and applications, publ. Bristol: Adam Hilger.

Cross, JA & Smith, P 1994, Electrostatic enhancement of water sprays for coal dust suppression (Interim Project Report, The University of New South Wales Department of Safety Science), Australian Coal Association Research Program Final Report, Project No. C1621, available Brisbane: Australian Research Administration Pty Ltd.

Cross, JA, Fowler, JCW & Xiao Fuchun 1998, Electrostatic enhancement of water sprays for dust suppression (Interim Project Report, The University of New South Wales School of Safety Science), Australian Coal Association Research Program Final Report, Project No. C4041, available Brisbane: Australian Research Administration Pty Ltd.

Law, SE 1978, 'Embedded-electrode electrostatic-induction spray-charging nozzle: theoretical and engineering design', *Transactions of the American Society of Agricultural Engineers*, vol. 21, no. 10, pp. 1096-1104.

Millipore 2001, *Laboratory Catalogue 2001 – 2002*, publ. Bedford, MA: Millipore Corporation.

SKC 2001, *Comprehensive Catalog and Air Sampling Guide*, International edn 2001/2002, publ. Eighty Four, PA: SKC.

Spraying Systems Co. 1994, Industrial Spray Products, Catalog 55M.

Xiao Fuchun 2000, Electrostatic charging of water sprays by corona and induction for dust suppression, unpublished PhD thesis, The University of New South Wales School of Safety Science.

This page intentionally blank